Temporal variability in potentially toxic elements (PTE's) and benthic Foraminifera in an estuarine environment in Puerto Rico

Article *in* Micropaleontology · May 2018

CITATIONS
0

READS
78

4 authors, including:

Michael Martinez-Colon
Florida A&M University
25 PUBLICATIONS **160** CITATIONS
SEE PROFILE

Joseph M. Smoak
University of South Florida
101 PUBLICATIONS **1,370** CITATIONS
SEE PROFILE

Temporal variability in potentially toxic elements (PTE's) and benthic Foraminifera in an estuarine environment in Puerto Rico

Michael Martínez-Colón[1], Pamela Hallock[2], Carlos R. Green-Ruíz[3] and Joseph M. Smoak[4]
[1] *School of the Environment, Florida A&M University, Tallahassee, FL, USA*
[2] *College of Marine Science, University of South Florida, St. Petersburg, FL, USA*
[3] *Unidad Académica Mazatlán, Instituto de Ciencias del Mar y Limnología, Universidad Nacional Autónoma de México, Mazatlán Sinaloa, México*
[4] *Environmental Science, University of South Florida, St. Petersburg, FL, USA*
email: michael.martinez@famu.edu

ABSTRACT: Bulk concentrations of PTEs (potentially toxic elements) were assessed and compared with foraminiferal assemblages from core sediments from TL (Torrecillas Lagoon), on the north coast of Puerto Rico. Temporal distributions of mud, Fe, Al (proxy for terrigenous sedimentation), and rhenium (proxy for anoxia) reflected changes in land use within the drainage basin associated with human activities over the past century. The mud-dominated sediments provided a major "sink" for PTEs, while Fe oxides and sulfides served as a secondary "sinks". Temporal variability of Re revealed intervals of aerobic *vs* anaerobic conditions in the lagoon. The dominant foraminiferal taxa, *Ammonia beccarii*, *Quinqueloculina rhodiensis*, *Quinqueloculina seminula*, and *Ammobaculites agglutinans*, coupled with low foraminiferal densities and species diversities, as well as barren samples, are characteristic of stressed estuarine environments. Overall bulk concentrations of Cu and Zn negatively correlated with foraminiferal absolute/relative abundances, diversity indices and incidences of test deformities. However, there are no correlations with the assumed bioavailable counterparts ($F2_{Tess}$-Cu and $F2_{Tess}$-Zn) were observed. These results indicate that fractionation of PTEs need to be considered in relation to their biological significance to foraminiferal ecology, which may differ substantially from bioavailability to metazoans that ingest sediments. The application of the acid-soluble $F2_{Tess}$ is not recommended in environmental studies using foraminifers as bioindicators, as PTEs in this fraction are likely not bioavailable to these protists.

Keywords: Heavy metals, Foraminiferal Ecology, Fractionation, Bioavailability, Hypoxia

INTRODUCTION

Estuaries are unique ecotones that provide habitat for numerous organisms, as well as ecosystem services including nursery and feeding grounds for developmental stages of neritic and coastal marine species. Unfortunately, in addition to natural stressors, these coastal ecotones receive copious amounts of pollutants as a consequence of industrialization and coastal urbanization (Balachandran et al. 2006; Zitello et al. 2008; Seshan et al. 2010; many others). Numerous studies worldwide have assessed estuarine resiliency in response to stressors such as sewage (Abu-Zeid et al. 2013) and PTEs (Martínez-Colón et al. 2009, 2018). Estuarine environments are well known as sinks of PTEs, organic pollutants, and more recently, microplastics (e.g., Ling et al. 2017; Sharma and Chatterjee 2017). In addition, PTE (re)mobilization and potential bioaccumulation are dependent upon solubility in seawater, salinity, type of organic matter among other factors (e.g., Martínez-Colón et al. 2009). The impacts of PTEs on macro-/microbiota are highly dependent on bioavailability, concentration, and duration and timing of exposure (Pinto 2003). As PTEs have long lasting effects on the overall health of an estuary, they impact the diversity and abundance of benthic foraminifers (Yanko et al. 1998; Martins et al. 2015), thereby providing useful bioindicators of such pollution.

The TL (Torrecillas Lagoon) in northern Puerto Rico is influenced by many point and nonpoint sources of pollution (e.g., sewage discharge, boat marinas, etc.) (text-fig. 1). Several studies have characterized and documented the presence of PTEs in sediments, water or tissue samples (fish, clams, etc.) along with anoxic conditions, high fecal coliform counts and excess of nutrients (Ellis and Gómez-Gómez 1976; Ellis 1976; Webb and Gómez-Gómez 1998; SJBE 2000; SJBE 2009; Martínez-Colón and Hallock 2010; and Martínez-Colón et al. 2018). Only two studies have documented organic pollutants (e.g. PCBs, Dieldrin, etc.) from surface and core sediments of TL (San Juan Bay Estuary 2000; Webb and Gómez-Gómez 1998). For example, Vistamar, Villa Carolina, and Round Hills sewage treatment plants discharged into Quebrada Blasina until 1986, when the effluents were redirected towards the Carolina Regional Sewage Treatment Plant (SJBE 2000). Raw sewage from the Vistamar collection system occasionally reaches TL due to overflow (SJBE 2000).

Ecological indicators allow assessment of environmental conditions and trends over time (Dale and Beyel 2001). Bioindicators of environmental stress in estuarine environments can be very useful in identifying sources of pollution (Pinto et al. 2009; Bouchet et al. 2012; Emrich et al. 2017). Over the past 50 years,

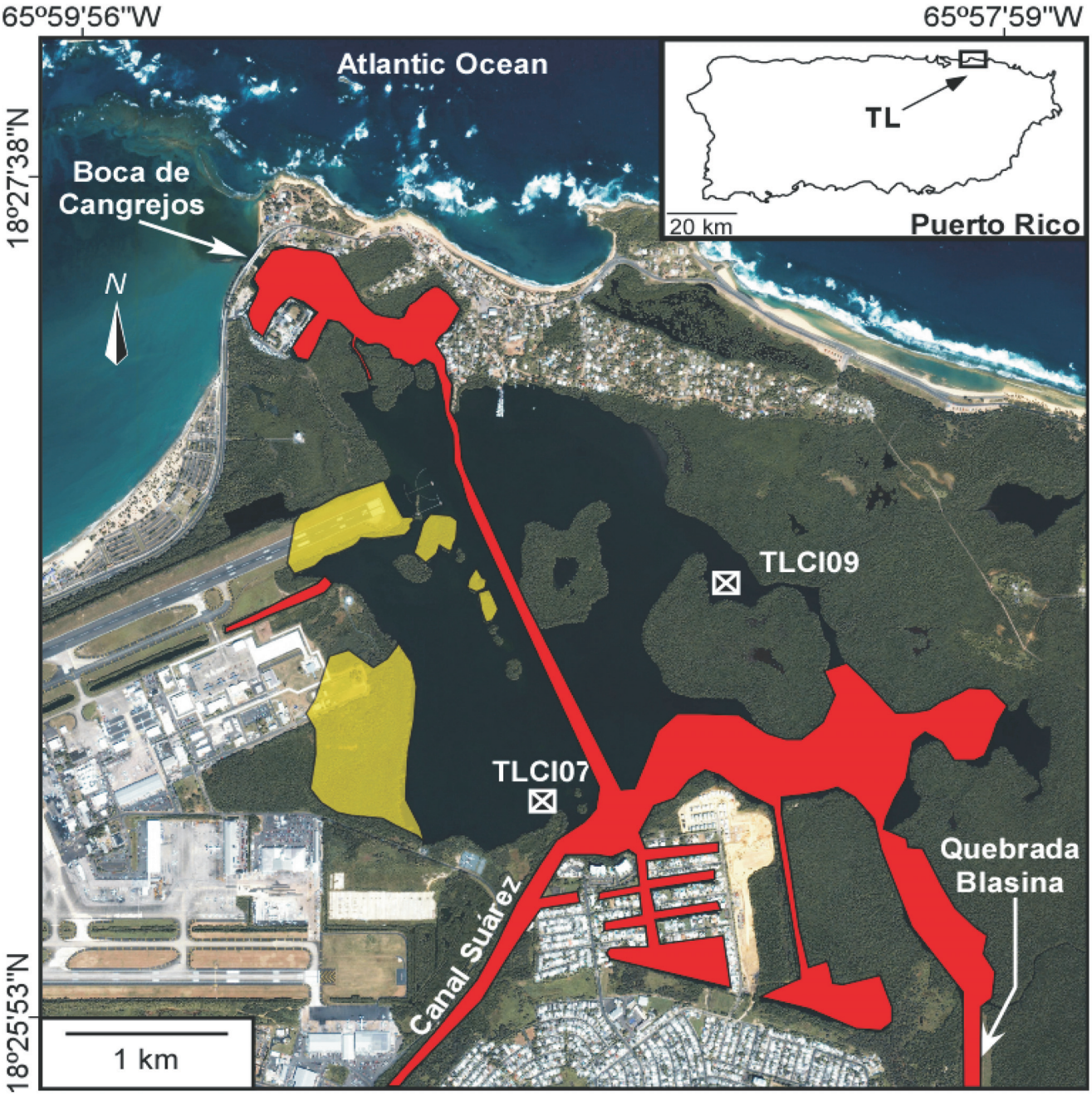

TEXT-FIGURE 1
Core sites in Torrecillas Lagoon (TL): TLCI07 and TLCI09. Insert: black arrow points to study area on the island of Puerto Rico. Red: dredging. Faded yellow: dredge spoil fill (from Ellis, 1976). Adapted from Martínez-Colón et al. (2018).

benthic foraminiferal assemblages have been used as pollution bioindicators (Martínez-Colón et al. 2009; Schönfeld et al. 2012; Sen Gupta 2013). Benthic foraminifers are sensitive to spatial/temporal environmental changes and their relatively rapid responses make them excellent sentinel organisms of pollution (e.g., Alve 1995; Martínez-Colón et al. 2009). For example test deformities are a biological response to stress. These deformities can be attributed to the incorporation of Cu^{+2} and other PTEs during biomineralization by potentially changing the crystalline structure of $CaCO_3$ (calcite) into other forms of the mineral (e.g., malachite). Moreover, benthic foraminifers, with inherently high surface-to-volume ratios, are potentially susceptible to PTE exposure associated with contaminated sediments and porewaters.

Changes in temperature, salinity, DO (dissolved oxygen), pH, sediment input, dissolved nutrients and organic carbon sources, and other natural and anthropogenic parameters influence

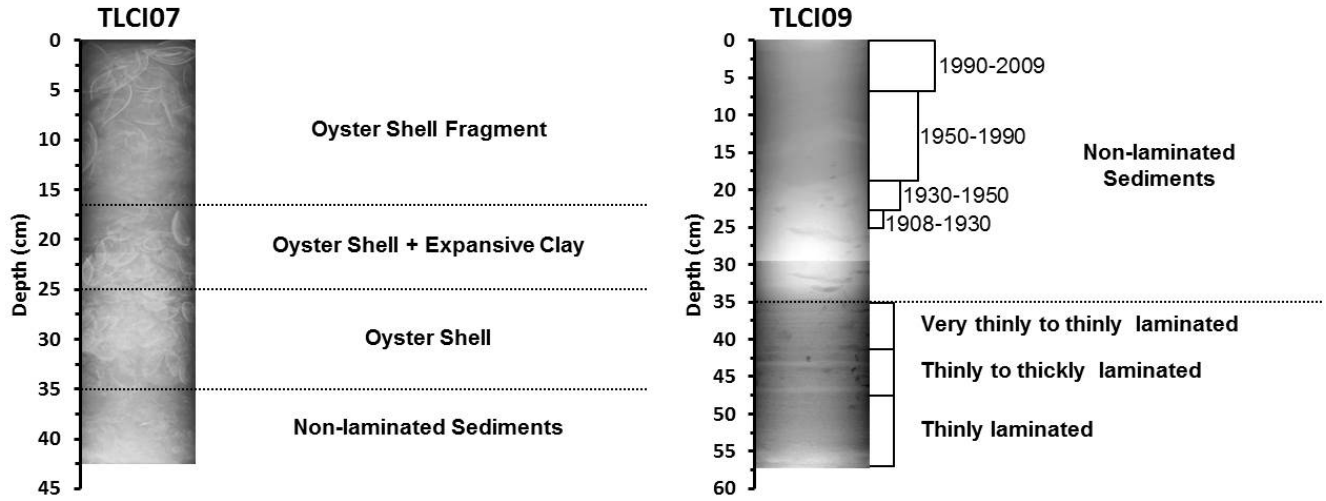

TEXT-FIGURE 2
Composite x-ray radiographs of cores TLCI07 and TLCI09.

foraminiferal assemblages (e.g., Martínez-Colón et al. 2009; Mateu-Vicens et al. 2014; Yanko et al. 2017). In estuarine environments in Puerto Rico, benthic foraminifers were first used as bioindicators of pollution by Seiglie (1968, 1971, 1974). In TL only three studies have previously assessed foraminiferal assemblage distributions and the dominance of *Ammonia becarii* and *Quinqueloculina rhodiensis* and their deformities as response signals of excess organic matter and PTE pollution coupled with sub- to anoxic conditions (Seiglie 1975b; Martínez-Colón and Hallock 2010; Martínez-Colón et al. 2018).

This research investigated the use of benthic foraminiferal assemblages as bioindicators of PTE pollution coming from sediment cores collected in TL. The objectives were to determine the distribution and bioavailability of PTEs in the cores to assess their influence on the temporal distributions of benthic foraminifers.

METHODOLOGY

Location

The SJBE (San Juan Bay Estuary) system, the largest estuary in Puerto Rico, comprises ~240 km^2 of land (drainage basin), of which 25 km^2 are submerged (Webb and Gómez-Gómez 1998). The SJBE system consists of semi-enclosed bays, lagoons, and natural and dredged channels (Martínez-Colón et al. 2018). Within the eastern subtidal portion of the SJBE system (text-fig. 1), TL has an average depth of 2.4 m and is influenced by sources of normal marine, fresh, and brackish waters (Gómez-Gómez et al. 1983).

The semidiurnal tidal range of TL is approximately 0.60 m (Bunch et al. 2000). The tidal regime has been impacted by dredging activities, resulting in increased residence times and increased volume of 110% compared to pre-dredging conditions (Ellis 1976). In several areas in TL, anoxic conditions (>3.5 m water depth), a well-defined halocline (1–2 m) and thermocline (0–6 m), and waters corrosive to $CaCO_3$ (>5 m; pH<7.4) have been documented (Martínez-Colón et al. 2018). These stratifications are attributed to disruption of circulation by dredging (Ellis 1976; Martínez-Colón et al. 2018), which impedes mixing and diffusion of oxygen, allowing slightly deeper areas to serve as "nutrient traps" (Ellis 1976). The average surface-water salinity (27 PSU), pH (7.9), temperature (32°C), and DO (6.9 mg/L) were recorded at the time of surface-sediment sampling describe by Martínez-Colón et al. (2018). Highest salinity (35 PSU) was recorded in the NE sector, while the lowest DO (0.6 mg/L) values were found towards the SE section of the lagoon.

Field Sampling

Sediment push cores (43–57 cm) were collected during sampling trips in June 2007 (TLCI07: 18°26'22"N, 65°58'59"W; 1.4 m water depth) and June 2009 (TLCI09: 18°26'52"N, 65°58'35"W; 12 m water depth) (text-fig. 1). Acid-washed polycarbonate core liners (10 cm diameter) were used to collect sediment cores. To minimize potential disturbances of sediments within the core barrel, excess tubing without sediment was removed. The top of the core was capped as close as possible to the sediment surface. Within three hours after collection, cores were frozen at -4°C. A YSI-probe was used to determine in situ water column temperature (°C), pH, salinity, and DO (mg/L) profiles during field sampling.

Laboratory Sample Preparation

Sediment Samples

Frozen cores were X-rayed to identify sediment stratification, structure, and potential bioturbation. The cores where subsequently thawed, extruded, placed into acid-washed (10% HCl solution) plastic Nalgene© containers, frozen, and subsequently freeze dried and subsampled. The following analyses were conducted on all subsamples: grain size, TOC (percent total organic carbon), CO_3 (percent carbonate content), bulk sediment PTE concentrations, and bioavailable PTE concentrations in the mud fraction. In this study, what is reported as "bioavailable" ($F2_{Tess}$-Cu, $F2_{Tess}$-Zn, $F2_{Tess}$-Fe) was the $F2_{Tess}$-CO_3 fraction based on operational "bioavailability" and defined as the second

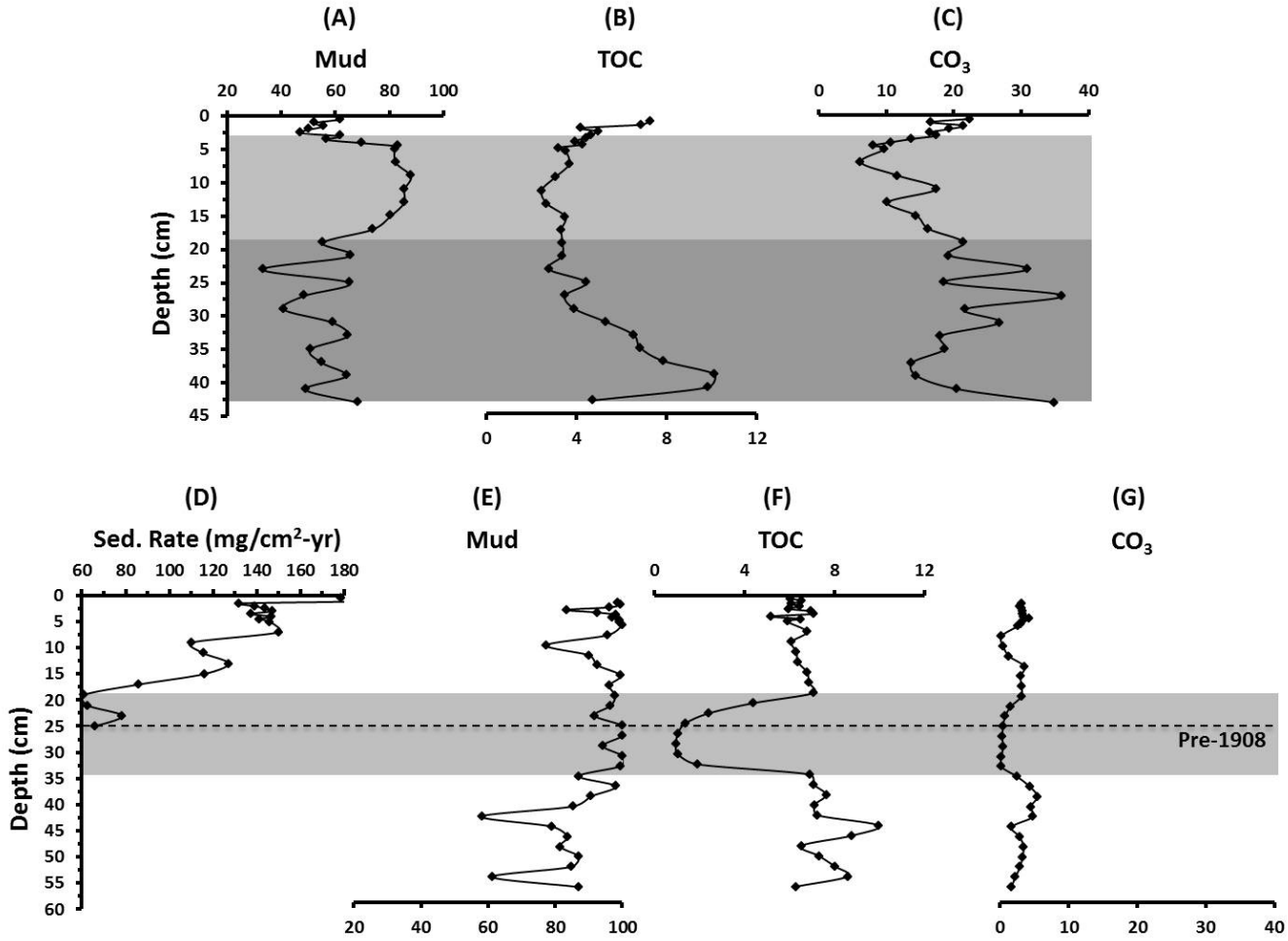

TEXT-FIGURE 3
Vertical distributions of Mud (percent mud), TOC (percent total organic carbon), and CO_3 (percent carbonate) in cores TLCI07 (A–C) and TLCI09 (D–G). Light gray bar: higher terrigenous influence. Dark gray bar: anoxic conditions.

most bioavailable fraction by Tessier et al. (1979). For sedimentation rates and dating, sampling resolution was 0.5 cm for the first 5 cm (Pb/Cs dating) and 2 cm intervals thereafter.

Grain size, TOC, CO_3, bulk and bioavailable PTE concentrations were analyzed following the protocols described in detail in Martínez-Colón et al. (2018). In summary, subsamples were wet sieved over a 63 µm mesh (assess mud-size sediments by weigh difference) and dried followed by standard sieving for grain size analysis. Units are expressed in phi (Ö). For TOC and CO_3, subsamples were analyzed by titration using a UIC Carbon Coulometer. For bulk PTE analyses, subsamples were sent to ACTLABS Laboratories Inc. (www.actlabs.com) in Canada for preparation and geochemical analysis (ICP-MS) of Cu, Zn, Ni, Pb, As, Li, Se, Fe, Mn, V, Re, and Al. For the acid-soluble concentrations of $F2_{Tess}$-Cu, $F2_{Tess}$-Zn, and $F2_{Tess}$-Fe, subsamples were analyzed by Atomic Absorption Spectroscopy.

Radiometric dating was achieved by measuring ^{210}Pb via gamma spectrometry and applying the CRS (Constant Rate of Supply) model which takes into account excess ^{210}Pb and sediment mass from each interval to determine mass accumulation rates and ages (Appleby 2001). This model is ideal in shallow systems such as TL where ^{210}Pb-supply is dominated by atmospheric input (Appleby 2001). For a detailed account of the procedures and instruments used for sample preparation and gamma counting, see Breithaupt et al. (2014) and Smoak et al. (2013).

Foraminiferal Samples

Subsamples of sediment were analyzed for total foraminiferal assemblages following the protocols described in Martínez-Colón et al. (2018). Freeze-dried sediment subsamples (sediment mass range 3.0–4.6 g [TLCI07]; 2.7–10.6 g [TLCI09]) were wet sieved (63 µm mesh) to remove clay particles and then dried at 50°C. Well preserved foraminiferal tests were picked until 160–300 individuals were counted. Specimens were identified using the generic taxonomy established by Loeblich and Tappan (1987) and to species level when possible, following Poag (1981) and Seiglie (1971, 1975a,b). The relative abundances of the dominant species assemblage were calculated as

TABLE 1
Depth, percent CO_3 (carbonate) and TOC (percent total organic carbon) for all samples.

Core Sample	Depth (cm)	CO_3	TOC	Core Sample	Depth (cm)	CO_3	TOC	Core Sample	Depth (cm)	CO_3	TOC
TLCI07#1	0.5	22	7	**TLCI07#28**	41	20	10	**TLCI09#25**	35	3	7
TLCI07#2	1	17	7	**TLCI07#29**	43	35	5	**TLCI09#26**	37	4	7
TLCI07#3	1.5	22	4					**TLCI09#27**	39	5	8
TLCI07#4	2	20	5	**TLCI09#1**	0.5	3	6	**TLCI09#28**	41	4	7
TLCI07#5	2.5	17	5	**TLCI09#2**	1	3	7	**TLCI09#29**	43	5	7
TLCI07#6	3	18	4	**TLCI09#3**	1.5	3	6	**TLCI09#30**	45	2	10
TLCI07#7	3.5	14	4	**TLCI09#4**	2	3	6	**TLCI09#31**	47	3	9
TLCI07#8	4	11	4	**TLCI09#5**	2.5	3	6	**TLCI09#32**	49	3	7
TLCI07#9	4.5	8	3	**TLCI09#6**	3	3	7	**TLCI09#33**	51	3	7
TLCI07#10	5	10	4	**TLCI09#7**	3.5	4	7	**TLCI09#34**	53	3	8
TLCI07#11	7	6	4	**TLCI09#8**	4	3	5	**TLCI09#35**	55	2	9
TLCI07#12	9	12	3	**TLCI09#9**	4.5	3	7	**TLCI09#36**	57	2	6
TLCI07#13	11	17	2	**TLCI09#10**	5	3	6				
TLCI07#14	13	10	3	**TLCI09#11**	7	0	7				
TLCI07#15	15	14	4	**TLCI09#12**	9	0	6				
TLCI07#16	17	16	3	**TLCI09#13**	11	1	6				
TLCI07#17	19	22	3	**TLCI09#14**	13	4	6				
TLCI07#18	21	19	3	**TLCI09#15**	15	3	7				
TLCI07#19	23	31	3	**TLCI09#16**	17	3	7				
TLCI07#20	25	19	4	**TLCI09#17**	19	3	7				
TLCI07#21	27	36	4	**TLCI09#18**	21	2	4				
TLCI07#22	29	22	4	**TLCI09#19**	23	1	2				
TLCI07#23	31	27	5	**TLCI09#20**	25	0	1				
TLCI07#24	33	18	7	**TLCI09#21**	27	0	1				
TLCI07#25	35	19	7	**TLCI09#22**	29	0	1				
TLCI07#26	37	14	8	**TLCI09#23**	31	0	1				
TLCI07#27	39	14	10	**TLCI09#24**	33	0	2				

the number of tests of each species divided by the total number of specimens in the subsample (ARA- *Ammonia beccarii*; QRA- *Quinqueloculina rhodiensis*; AmRA- *Ammobaculites agglutinans*; and QsRA- *Quinqueloculina seminula*). Absolute abundances for all the species refer to number of tests per gram found in a subsample.

Data Analysis

For diversity indices and statistical tools, the protocols described by Martínez-Colón et al. (2018) were implemented. In summary, the parameters assessed include: (1) S (Species richness); (2) FD (Foraminiferal Density); (3) H(S) (Shannon Index); (4) E (Equitability Index); and (5) DF (Deformed Foraminifers). Hierarchical cluster analysis was performed on foraminiferal data, after adjustments for distribution and transformations (fourth-root) to determine ecological assemblages as described in Martínez-Colón et al. (2018).

The PTE data were assessed following the protocols of Acevedo-Figueroa et al. (2006) for EF (enrichment factor):

$$EF = ([M]_i / [E]_i)_{sediment} / ([M]_r / [E]_r)_{earth's\ crust}$$

Where M_i is the PTE concentration and E is the concentration of the normalizing element (Al) in sediment; M_r and E_r are the PTE and normalizing element (Al) concentrations in the Earth's crust. Although Abrahim and Parker (2008) demonstrated the utility of using the pre-industrial concentrations of the normalizing element from the studied area, our temporal data in both cores were not sufficiently clear to assign a local baseline of pre-industrial values for Al. For this reason, the PTEs were normalized for the average Al concentration found in shales, which are considered a world-wide standard reference guide for unpolluted sediments (Ekengele et al. 2008).

The EF index determines the relative incorporation of PTEs into the sediments. Values calculated represent the number of times the concentration of the PTE is above background level (Green-Ruíz et al. 2005). Values of EF <1 show "no enrichment"; 1–3 "minor enrichment"; 3–5 "moderate enrichment"; 5–10 "moderate severe enrichment"; 10–25 "severe enrichment"; 25–50 "very severe enrichment; and >50 "extremely severe enrichment" (Acevedo-Figueróa et al. 2006).

Pearson correlation analysis was performed using PRIMER© (v. 6) statistical software (Clarke and Gorley 2006) to determine if any significant trends were found based on log-transformed data (Parker and Arnold 1999). Pearson correlation analyses included mud, TOC, and CO_3, bulk PTE concentration,

$F2_{Tess}$-bioavailable copper ($F2_{Tess}$-Cu), zinc ($F2_{Tess}$-Zn), and iron ($F2_{Tess}$-Fe) concentrations, foraminiferal species absolute and relative abundances, S, FD, H(S), E, and DF.

RESULTS

Core Description

Core TLCI07, with a maximum length of 43 cm, was collected at a water depth of 0.65 m. A radiograph image of the core revealed four distinctive sedimentary "units" (text-fig. 2). The lower facies, which represent anoxic conditions, and consists of three units: Unit 1, observed between 43–35 cm, consisted of non-laminated sediments; Unit 2 is an oyster-shell layer between 35–25 cm depth; and Unit 3 consisted of a layer of oyster shell fragments in plastic clay at the 25–19 cm depth interval. The upper facies, which represent oxic conditions, consists of Unit 4 which is a layer of shell fragments mixed with mud between 19–0.5 cm.

Percent mud fluctuated between 33–68% between 43–19 cm depth (text-fig. 3a). From 19 cm upward, a consistent increase was observed, peaking at 86% at 9 cm depth, decreasing to 47% above that maximum. The highest TOC was 10.1% at 39 cm (Table 1), decreasing four-fold from core-base to core-top (text-fig. 3b). The CO_3 fraction varied from 6–36% (Table 1), with highest percentages in the lower facies where oyster shell fragments were visually dominant (text-fig. 2), with lower percentages above 30 cm depth in the core (text-fig. 3c).

Core TLCI09, with a maximum length of 57 cm, was collected at a water depth of 12 m. A radiograph image of the core showed two distinctive sedimentary "units". The lower facies consisted of laminated sediments between 53–33 cm (Unit 1). The upper facies consist of Unit 2 which is comprised by non-laminated sediments although this could be an overexposure artifact of the radiograph due to excess ice that masked laminations. Based on PTE, TOC, and CO_3 distributions, two distinct intervals are observed between 33–19 cm (intermediate) and 19–0.5 cm (upper).

All samples were mud dominated. The variability was minimal (77–100%) through most of the core (text-fig. 3e). Below 43 cm, mud was somewhat more variable. The TOC values ranged from 1–10% (Table 1) with values as low at 1% in the 35–19 cm depth interval, and values of ~6% at both the core base and core top (text-fig. 3f). The CO_3 was consistently <6% (Table 1, text-fig. 3g).

Only Core TLCI09, sampled on May 22, 2009, provided reliable sedimentation rates and ages. Calibrated dates for the core ranged from 2009 (0–0.5 cm interval) to 1908 (23–25 cm interval), with average mass-sedimentation rate of 124 mg/cm^2-yr (text-fig. 3d). Due to possible bioturbation, no earlier ages were determined. All raw data and calculated dates are presented in Appendix A (supplemental material).

Potentially Toxic Element Distribution in Sediments

Twelve PTEs were assessed for bulk concentrations. Only Cu, Zn, and Fe were considered for bioavailability, since Cu and Zn previously have been correlated with foraminiferal assemblage changes in field and culture studies; Fe was selected due to its significance as a redox indicator.

Raw data for all core samples (TLCI07 and TLCI09), including their respective EF and bioavailable concentrations, are found in Appendix B (supplemental material).

Torrecillas Lagoon Core TLCI07

Temporal distributions of PTEs are shown in text-figure 4. Copper, Zn, Ni, Pb, Li, Fe and V all showed peaks in the 3–19 cm core interval, consistent with the highest mud and Al (text-figs. 3a and 4l). Other noticeable trends include in the stratigraphic distribution of As, Se and Re, with peaks at ~35 cm depth (text-figs. 4e, 4g, and 4k), which were consistent with TOC (text-figs. 3b). Manganese generally increased from core-base to core-top (text-fig. 4i).

The ERL (Effects range low) criteria, as defined by Long et al. (1995), were only available for Cu (34–270 ppm), Zn (150–410 ppm), Ni (20.9–51.6), Pb (46.7–218), and As (8.2–70) (text-fig. 4). Copper and As were both consistently above the ERL concentrations, Zn and Pb were below, and Ni exceeded the defined ERL at its peak in the 3–19 cm depth range.

Relative to EF, Ni and Li show "no enrichment" while other bulk PTE concentrations indicated "minor enrichment" of Cu, Zn, V, Fe, Mn (text-fig 5). Selenium and As decreased upcore. Their concentration range from "moderate-severe enrichment" to "no enrichment" from 43–11 cm. A rapid increase towards "moderate-severe enrichment" and "minor enrichment" of As and Se, respectively (text-fig 5) occurred from 11–0.5 cm. From core-base to core top, Pb distribution reveal "no enrichment" except for a spike to "moderate-severe enrichment" at 2.5 cm.

Aluminum concentrations range from 3.7–6% below 19 cm depth in the core (text-fig. 4l). A consistent upcore increase from 19 cm reaching a maximum value of 9.7% at a depth of 11 cm is observed. Its concentration decreases to 3.7% at a depth of 3 cm. The concentrations of Re range from 0.009–0.081 mg/kg (text-fig. 4k). The overall distribution trend of Re throughout the core (base: 0.05 mg/kg; top: 0.02 mg/kg) was similar to that of TOC, As and Se, but opposite to Mn and V. As a conservative element in the oceans, Re concentration in sediments increases when sequestered by organic material. In this study, Re was used as an indicator of anoxic conditions.

Acid-soluble fractions of only three PTEs were assessed to indicate bioavailability, and all revealed similar temporal distributions. The $F2_{Tess}$-Cu and $F2_{Tess}$-Zn had a 10-fold and two-fold increase in concentrations ranging from 1.50–15.8 mg/kg and 7.93–17.31 mg/kg respectively from core-base to core-top (text-fig. 4a and 4b). Both acid-soluble and bioavailable PTEs reached maximum concentrations at 13 cm similar to their bulk concentration counterparts. The $F2_{Tess}$-Fe ranged in concentrations between 0.23% (43 cm) and 0.79% (25 cm) (text-fig. 4h).

A Pearson correlation matrix (Appendix C, supplemental material) was calculated for the 10 PTEs of concern, including acid-soluble PTE fractions ($F2_{Tess}$-Cu, $F2_{Tess}$-Zn, $F2_{Tess}$-Fe), TOC, CO_3 and mud. Zinc, Ni, Li, Fe, and V are all significantly correlated with mud. Copper with a correlation coefficient of 0.35, as compared to 0.37 at 95% confidence, is also weakly correlated with mud. Arsenic is the only PTE that shows strong negative correlation with mud. Most PTEs except for As, and Se are negatively correlated with TOC. None of the acid-soluble fractions correlated with CO_3 or mud. Carbonate content correlated negatively with Pb, Fe and V and positively with As.

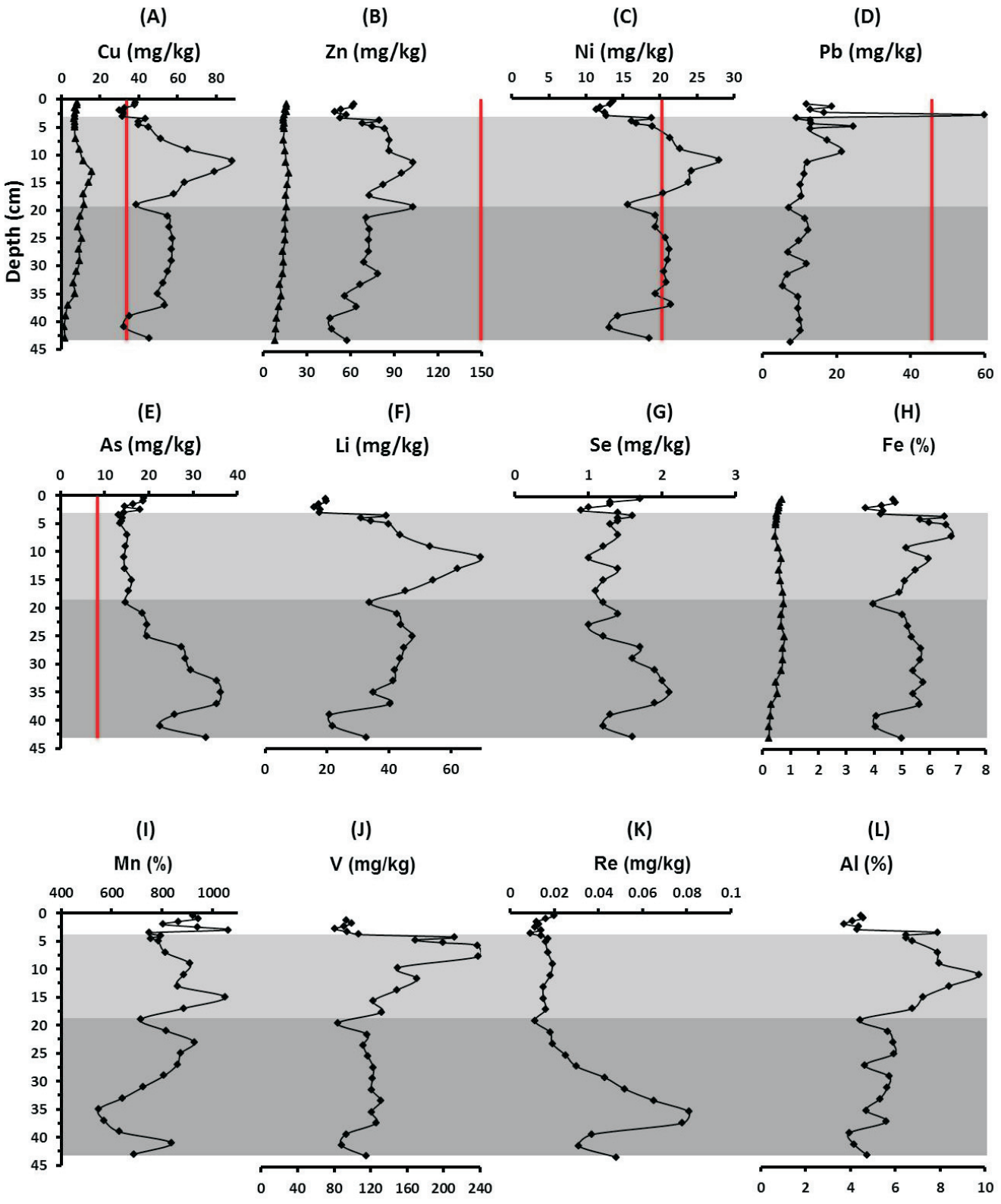

TEXT-FIGURE 4
Temporal distributions of PTEs in core TLCI07. Triangle: $F2_{Tess}$-Cu, $F2_{Tess}$-Zn, and $F2_{Tess}$-Fe bioavailable concentrations. Diamonds: bulk PTE concentrations. Light gray bar: interval of higher sedimentation. Dark gray bar: interval of anoxic conditions. Red line: ERL (Effect range low) values as defined by Long et al. (1995).

Torrecillas Lagoon Core TLCI09

Temporal distributions of PTEs are shown in text-figure 6. Copper, Zn, Ni, Fe, and V (text-figs. 6a–c, 6h, and 6j) reveal similar strong peaks from ~19–35 cm interval, which are consistent with the lowest mud and highest Al percentages (3.84–10%) (text-figs. 3e, 6l). Lithium, Se, and Re declined at the same interval, as did TOC and CO_3 (text-figs. 6f–g, 6k, 3f–g). Lead steadily declined from core-base to 35 cm, then remained consistently low to the core-top while As and Mn showed no discernable trend except for their highest values being at 19 cm depth (text-figs. 6d–e, 6i).

Nickel exceeded the defined ERL concentration at its peak in the 19–35 cm core interval. Relative to EF, the concentrations of Ni, Li, Mn, As showed "no enrichment" while Cu, Zn, V, Fe, Se indicated "minor enrichment" (text-fig. 7). Lead decreased upcore from "moderate enrichment" to "minor enrichment with "no enrichment" at 19–35 cm depth.

Aluminum concentrations range from 3.8–10% (text-fig. 6l). Starting at 35 cm depth, consistent increase with a maximum value of 10% at 31–25 cm depth interval, was observed from the base of the core at depth 35 cm. The concentration decreased to a minimum of 5.27% at a depth of 15 cm. The Re the concentrations range from 0.0005–0.0170 mg/kg (text-fig. 6k). A strong decrease in concentration for Re occurred within the 19–35 cm interval, mimicking the pattern of TOC (text-fig. 3f).

The three acid-soluble fractions ($F2_{Tess}$-Cu, $F2_{Tess}$-Zn and $F2_{Tess}$-Fe) showed very similar temporal distributions resembling that of Al. The $F2_{Tess}$-Cu range in concentrations from 2–41 mg/kg (text-fig. 6a). The $F2_{Tess}$-Zn and $F2_{Tess}$-Fe concentrations range from 42–79 mg/kg and 1.05–2.56% respectively (text-fig. 6b, 6h).

A Pearson correlation matrix (Appendix D, supplemental material) was calculated for the 10 bulk PTEs, acid-soluble fractions of PTEs ($F2_{Tess}$-Cu, $F2_{Tess}$-Zn, $F2_{Tess}$-Fe), TOC, CO_3 and mud. No PTE significantly correlated with mud at the 95% confidence. Except for a negative correlation with Pb, none of the PTEs significantly correlated with mud at the 95% confidence intercal. Copper, Zn, Ni, Fe, and V negatively correlated with TOC and CO_3. Lead, Li and Se positively correlated with TOC and LI and Se with CO_3. $F2_{Tess}$-Zn was the only acid-soluble bioavailable PTE fraction that is positively correlated with TOC.

Foraminiferal Assemblages

Torrecillas Lagoon Core TLCI07

From 29 sediment subsamples, 6,893 benthic foraminifers representing 12 genera and 21 species were picked and identified (Appendix E- supplement material). Of the 20 species present in at least 5% of the subsamples, *A. beccarii* (4,567 individuals), *A. agglutinans* (574 individuals), *Q. rhodiensis* (464 individuals), *Elphidium discoidale* (352 individuals), and *Triloculina* sp. (261 individuals) were the most abundant taxa across all samples. None of the other species accounted for 100 individuals across all samples.

Text-figures 8a–c show the temporal variability of the relative abundances of the three most abundant taxa. *Ammonia becarii* (ARA) was consistently dominant in the lower facies (69–89%), increasing somewhat up to 23 cm depth, followed by a strong decrease to a minimum value of 37% at 2.5 cm. *Ammobacculites agglutinans* (AmRA) and QRA show the opposite trends, with lows below 23 cm, then increasing towards the core top. *Quinqueloculina rhodiensis* was the most abundant miliolid.

Except for three subsamples devoid of foraminiferal tests, species richness ranged from 8–13 species (text-fig. 9a), while FD was consistently at ~60 tests/g (text-fig. 9b). The trends in diversity [H(S)] and DF (text-figs. 9c–d) reflected the trends in AmRA and QRA, as did the E index to some extent. Deformities of foraminiferal tests were found in 25 out of 29 samples, occurring in up to 16% of the specimens identified in a sample. Nearly all deformities were observed in miliolids except for two samples in which deformed *A. beccarii* tests were found.

Foraminiferal cluster analysis (Bray-Curtis similarity) revealed only three clusters. Cluster 1 was the overwhelmingly dominant *A. beccarii*, while Cluster 2 was composed of *A. agglutinans*, and *Q. rhodiensis*. Cluster 3 includes other common nearshore and estuarine taxa.

A Pearson correlation matrix (Appendix F, supplemental material) was calculated for the 10 PTEs, including bioavailable elements ($F2_{Tess}$-Cu, $F2_{Tess}$-Zn, $F2_{Tess}$-Fe), as well as TOC, CO_3, mud, foraminiferal taxa absolute abundances, ecological indices, relative abundances and percentages of test deformities. Several genera correlated either positively or negatively with PTEs and the other sediment characteristics examined, while none correlated with Fe, V, or TOC. Very weak correlations were found between the acid-soluble PTEs and foraminiferal taxa or their ecological indices except for a notable significant negative correlation with two *Elphidium* species. Absolute and relative abundances of *A. beccarii* positively correlate with Cu, Zn, Ni, As and Li, and negatively with Pb. *Ammobaculites agglutinans* correlate positively with Pb and Mn, and *Q. rhodiensis* with Pb. Both species and their percent deformed tests show negative correlations with Cu, Ni, As, Li and CO_3. Species richness negatively correlated with Pb, while H(S) and E correlated positively with Pb [H(S) also positively with TOC], and negatively with Cu, Zn, Ni, and Li [H(S) also negatively with $F2_{Tess}$-Cu and $F2_{Tess}$-Fe].

Torrecillas Lagoon Core TLCI09

A total of 33 subsamples examined in the core yielded only 750 foraminiferal specimens, which were picked and identified as belonging to 13 genera and 23 species (Appendix G, supplemental material). Of the 17 species present in at least 5% of the subsamples, *Q. seminula* (181 individuals), *A. beccarii* (174 individuals), and *Q. rhodiensis* (139 individuals) were the most abundant species. None of the other species accounted for more than 70 specimens across all samples.

Thirteen subsamples, all with very low CO_3 values (<3%), were barren of foraminiferal tests (text-fig. 3g). The low foraminiferal counts and numerous barren samples produced no discernable temporal patterns (Appendix G, supplemental material). As a consequence, no temporal plots of ecological indices or abundances of dominant taxa were included. Species richness ranged from 0–13 species, while FD had a maximum value of 23 tests/g at 1 cm depth. Test deformities (0–7%) were found in only seven subsamples. The temporal variability of QsRA, ARA, and QRA also showed no discernable patterns. Cluster analysis again yielded three clusters: Cluster 1 was composed of

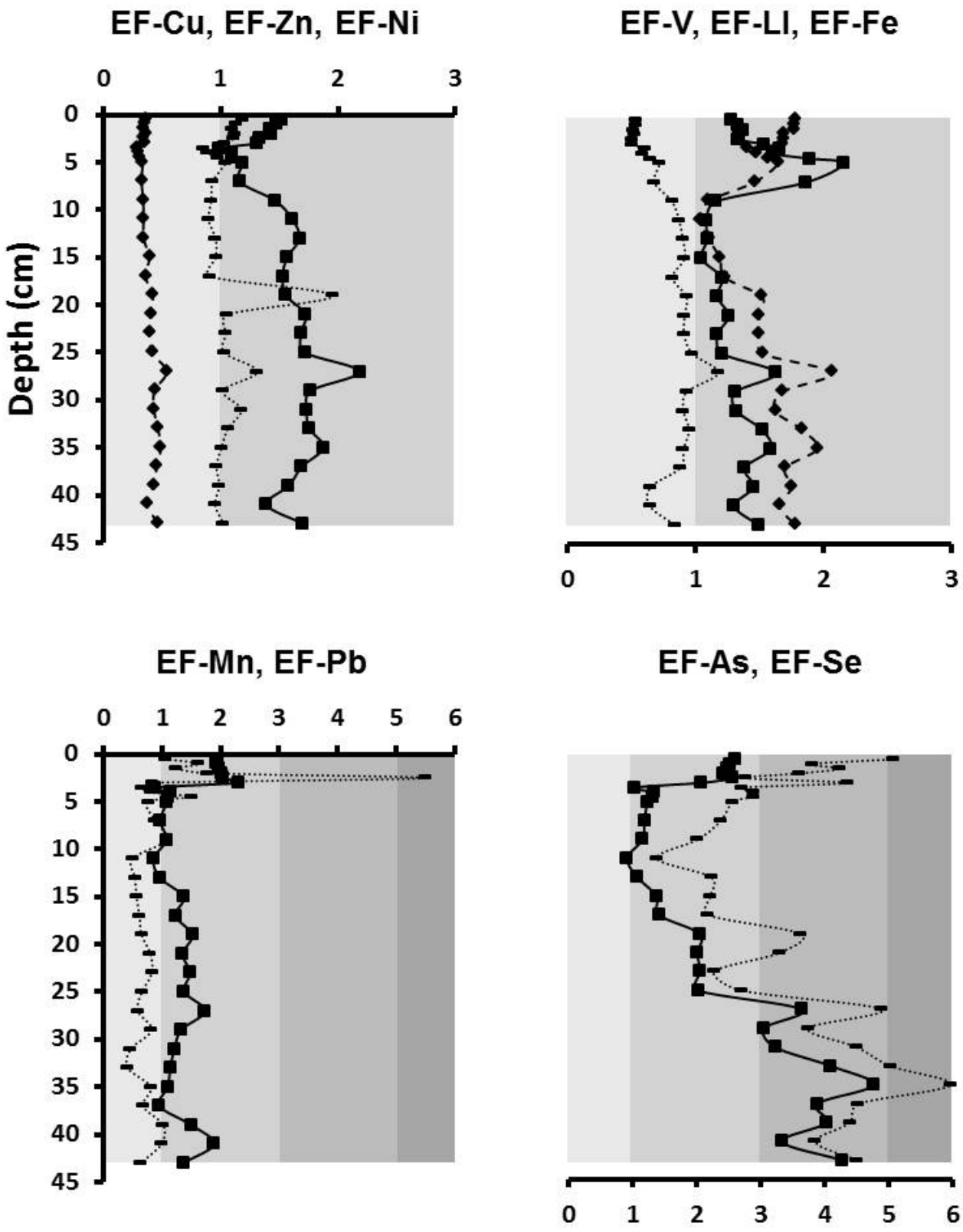

TEXT-FIGURE 5
Vertical distributions of EF (enrichment factors) in sediment core TLCI07. Range values: "no enrichment" (very light gray); "minor enrichment" (light gray); "moderate enrichment (gray); "moderate-severe enrichment (dark gray). Square, dash, and diamond symbols represent the first, second and third PTE in each panel.

Q. seminula and *A. beccarii,* Cluster *2* was only *Q. rhodiensis*, while Cluster 3 included the other species.

As with TLCI07, a Pearson correlation matrix (Appendix H, supplemental material) was calculated. As expected, relatively few significant correlations were identified among the studied parameters. Arsenic, Li and Mn are the only PTEs that are positively correlated with multiple taxa. Among the dominant taxa, only *Q. rhodiensis* absolute abundances correlated positively with As and Mn and the QRA with Li. Percent test deformities, S, and H(S) positively correlated with As, Li, and Mn. Zinc is the only PTE that is negatively correlated with S, H(S), and E.

DISCUSSION

Torrecillas Lagoon Core (TLCI07)

Potentially Toxic Elements in Sediments

From core base to top, two distinct facies observed from 43–19 (lower, <60% mud) and 19–4 cm (upper, >60% mud) (text-fig. 3A) were reflected in the distributions of PTEs, TOC, CO_3 and benthic foraminiferal tests. At a depth of ~35 cm in the core, the redox-sensitive element Re peaked, as did TOC, As and Se (text-fig. 4k). Rhenium, which is a conservative element in the water column, precipitates and increases in concentration in sediments under anoxic conditions (Seshan et al. 2010; Hastings et al. 2016; Schwing et al. 2016). In the case of the TL, water column stratification and poor circulation (e.g., Martínez-Colón et al. 2018), coupled with relatively abundant organic matter, promote anoxia as supported by the presence of framboidal pyrite within the tests of foraminifers. Pyrite precipitation can indicate post-mortem exposure to anoxia (Buzas-Stephens and Buzas, 2005). Both Mn and CO_3 exhibit minima in the same section of the lower facies where Re peaked.

The muddier upper facies (19–4 cm) reflected increased erosion in the watershed and greater terrigenous input into TL. This conclusion is supported by the almost identical patterns between mud and Al (text-fig. 3a, 4l), with a close resemblance also with Fe (text-fig. 4h). Aluminum and Fe have been used as proxies for lithic/terrigenous sedimentation as these are dominant components of aluminosilicate (e.g., kaolinite) and ferromagnesian (e.g., biotite) minerals. Within the drainage basin of SJBE, 55 km^2 are covered by plutonic and volcaniclastic rocks (Webb and Gómez-Gómez 1998), which strongly suggests that the mud fraction in TL has an allochthonous lithic provenance. The variability in Al and Fe has been used by Larson et al. (2015) as sedimentologic signatures of runoff/rainfall events in St. John Island (US Virgin Islands). The increase in mud is likely a response to landscape alterations by anthropogenic activities since the 1800's. Similar changes in sedimentation patterns towards terrigenous muds, coupled with a decrease in TOC and CO_3, have been documented in similar environments in St. John Island's Coral Bay as being linked to landscape alterations by humans (Brooks et al. 2007).

Concentrations of Cu, Zn, Ni, Pb, Li, and V are elevated in the upper, mud-rich facies (text-fig. 4). Since PTEs readily adsorb to mud-sized sediment surfaces, muds appeared to provide a "sink" for these contaminants. Mud-bound PTEs can be bioavailable to foraminifers, since these contaminants can be readily desorbed or scavenged when minor changes in salinity or pH occur (Martínez-Colón et al. 2009; Martínez-Colón et al. 2018). Moreover, iron oxide formation under oxic/suboxic conditions (Davies et al. 2005) in the upper facies provides an ancillary "sink" for Cu, Zn, Ni, Li, Se, and V, thereby reducing their bioavailability (Tessier and Campbell 1987). This mechanism, associated with the sediment redox boundary layer, has been observed in estuaries elsewhere (e.g., Lee and Cundy 2001; Kalaivanan et al. 2017). The temporal variability of Se might have resulted from sequestration by Fe oxides (text-fig. 4) in the upper facies. Martínez-Colón et al. (2018) noted that PTEs that correlated positively with Fe/Mn in TL surface sediments indicated oxic/anoxic boundary conditions, in which significant fractions of these contaminants co-precipitated with Fe/Mn geochemical phases. In the lower anoxic facies, all PTEs were sequestered by Fe sulfides (e.g., FeS_2- pyrite). Similar observations were reported by Kalaivanan et al. (2017) in a tropical estuary in India in which they concluded that Fe/Mn oxide cycling at the sediment redox boundary is responsible for PTE sequestering and re-precipitation. Overall, the highest PTE concentrations were found intimately associated with mud as the dominant "sink" in the upper facies. As expected, $F2_{Tess}$-Cu, $F2_{Tess}$-Zn, and $F2_{Tess}$-Fe bioavailable PTEs show no discernable patterns between facies except for relative minor upcore increases (text-fig. 4).

Despite the multiple pollution sources in TL, PTE enrichment was surprisingly limited. The PTEs showing "minor enrichment" (Cu, Zn, V, Fe, Mn) indicated that the sources of these contaminants have not changed substantially over time. Lead showed "no enrichment" except for a "minor enrichment" incursion at 2.5 cm depth (text-fig. 5). This could be attributed to either laboratory procedure error or a short-term input of Pb. The latter is a more likely scenario because a constant decreasing enrichment can be observed towards the core top. The upcore decline in As (text-fig. 5) may reflect the reduction in agricultural activities; As was used as a bleaching agent for sugar processing (Webb and Gómez-Gómez, 1998).

Foraminiferal Distributions

The foraminiferal assemblages in TL are characteristic of estuarine environments, and temporal variability reflects environmental conditions at the sediment/water interface. The dominant species *A. beccarii*, *A. agglutinans* and *Q. rhodiensis* reflect the isolation of the core site from normal marine conditions (text-fig. 1). Numerous species in the genus *Ammonia* have been shown to be exceptionally resilient to environmental stressors, including variations in salinity, temperature, DO and many sources of PTE pollution, especially under nutrient pollution where labile organic matter is abundant (e.g., Seiglie 1968; Sen Gupta et al. 1996; Jorissen 1999; Unlu et al. 2006; Frontalini and Coccioni 2008; Geslin et al. 2014; Arslan et al. 2017; Yanko et al. 2017). Organic pollution is a common thread in estuarine environments in Puerto Rico, from which studies have found *A. beccarii* as the dominant taxon (e.g., Seiglie 1971; Martínez-Colón and Hallock 2010; Martínez-Colón et al. 2018).

Most species of the genus *Quinqueloculina* are characteristic of open-marine systems and tend to be pollution sensitive (Rao and Rao, 1979; Murray 1991; Badawi and El-Menhawey 2016). However, *Q. rhodiensis* and *Q. seminula* are quite stress tolerant and have been found thriving in the same environments as *A. beccarii* (Seiglie 1968, 1971; Martínez-Colón and Hallock 2010). Similarly, *A. agglutinans* has been reported to be a dominant taxon in environments with abundant organic matter in

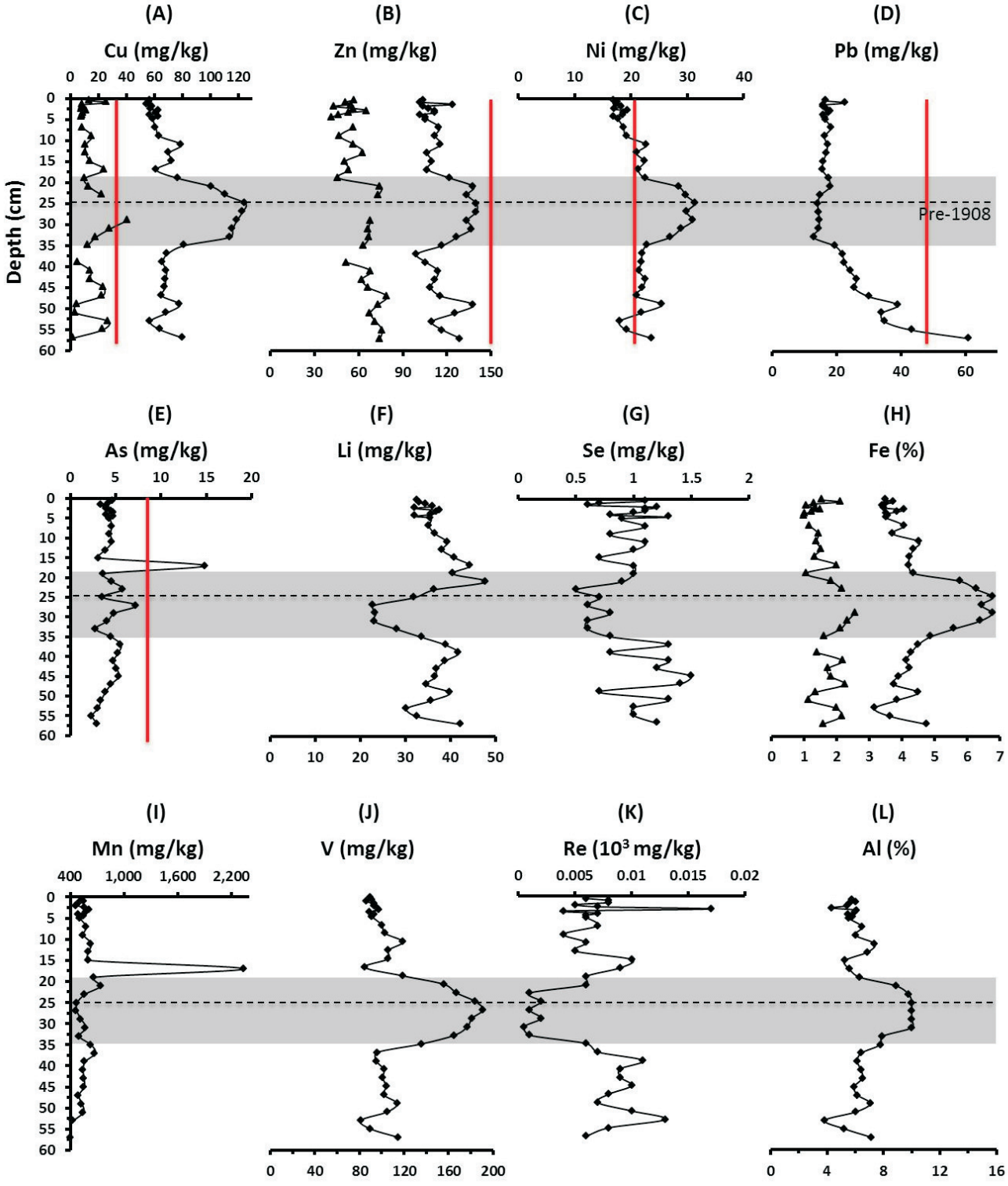

TEXT-FIGURE 6
Vertical distributions of PTEs in core TLCI09. Triangle: $F2_{Tess}$-Cu, $F2_{Tess}$-Zn, and $F2_{Tess}$-Fe bioavailable concentrations. Diamonds: bulk PTE concentrations. Light gray bar: interval of higher sedimentation. Red line: ERL (Effect range low) values as stipulated by Long et al. (1995).

Puerto Rico (Seiglie, 1968) and in Kuwait (Al-Zamel et al. 2009).

The variability of the ecological indices throughout the core was relatively similar to that recorded in surface samples from TL (see Martínez-Colón et al. 2018). Species richness, FD, H(S) and E were consistently low, indicative of impacted and stressed environments (e.g., Schafer et al. 1991; Yanko et al. 1998). Minimal differences in S observed in the core (text-fig. 9a) indicate persistently stressed conditions in the lagoon. Oxic/anoxic conditions do not fully explain the overall low values although studies have found similar numbers associated with high organic matter content (Donnici et al. 2012; Foster et al. 2012). Of all the PTEs studied, Pb was the only contaminant having a negative correlation with S. Since Pb was positively associated with TOC, Pb complexed with organic matter might serve a stressor due to its higher bioavailability.

The abundance of foraminiferal tests in the core samples (FD) varied minimally (52–77 individuals/g). Interestingly, FD correlated positively with Cu, Ni, As, Li, and Se, some of which have been previously reported to influence foraminiferal distributions (e.g., Donnici et al. 2012; Koufri et al. 2005; Martins et al. 2011; Martins et al. 2013). However, bulk concentrations of PTEs should be interpreted cautiously, as they can provide an overestimation of impact on foraminiferal assemblages, and bioavailability depends upon chemical fractionation (Martínez-Colón et al. 2009, 2018). This is important to consider since there is no clear consensus on what chemical fractions are bioavailable to the foraminifers (Martínez-Colón et al. 2018).

Higher H(S) and E values in the upper facies indicate that conditions in the lagoon have improved slightly for the foraminifers (text-fig. 9c). However, even the "improved values" are still low and are typical of environments influenced by stressors (e.g., Bergin et al. 2006; Foster et al. 2012; Schintu et al. 2016). Negative correlations with several PTEs, including $F2_{Tess}$-Cu and $F2_{Tess}$-Fe, could implicate these PTEs in stressing the foraminiferal assemblages, as interpreted in other studies (e.g., Martins et al. 2015; Schintu et al. 2016). However, as noted above, bulk PTE concentrations potentially overestimate their impacts since the reported values can include multiple chemical fractions (e.g., exchangeable, acid-soluble, reducible, oxidizable, and residual) (Martínez-Colón et al. 2018) as seen by the positive correlation and lack thereof between *A. beccarii* with Cu/Zn, $F2_{Tess}$-Cu, and $F2_{Tess}$-Zn. Similarly, the $F2_{Tess}$-Cu and $F2_{Tess}$-Fe could not have a direct effect on foraminiferal assemblages and distributions since these pollutants are bounded to the crystalline structure of carbonates and becoming less bioavailable.

The increase in diversity [H(S)] upcore reflects the increased prevalence of *Quinqueloculina* and *Ammobaculities* (text-figs. 9c, 8b–c). Moreover, since deformed tests were found mostly in miliolid taxa, including *Quinqeloculina*, the upcore increase in DF reflects the upcore increase in QRA. These observations could be interpreted as improvements in the environmental conditions, such as higher or more stable salinity and dissolved oxygen, which allowed miliolid taxa to survive, but demonstrate stress through test abnormalities. This interpretation is supported by the overall decreasing trends of *A. beccarii* and *Elphidium* sp., which are known indicators of stressed conditions. Note that the absolute and relative abundances of *A. beccarii* positively correlated (and negatively in the case of *A. agglutinans* and *Q. rhodiensis*) with Cu, Zn, and Fe and not with the bioavailable counterparts ($F2_{Tess}$-Cu, $F2_{Tess}$-Zn, $F2_{Tess}$-Fe). While previous studies have concluded that bulk PTE concentrations can be foraminiferal stressors (e.g., Alve, 1991; Fontanier et al. 2012; Schintu et al. 2016), as noted by Martínez-Colón et al. (2018), future studies to determine the functional bioavailability to the foraminifers, instead of relying on previously defined operational bioavailability (Tessier et al. 1979; Bacon and Davidson, 2008; Zimmerman and Weindorf, 2010), are critically needed to fully understand inconsistent results.

Torrecillas Lagoon Core (TLCI09)

Potentially Toxic Elements in Sediments

Mud was overwhelmingly dominant in the TLCI09 core (text-fig. 3e), and is consistent with a sheltered environment (text-fig. 1). The TOC decreased between 35–19 cm (text-figs. 3f–g). The low CO_3 in the sediment (<5%) may reflect the corrosive environment in this relatively deep location (12 m); Martínez-Colón et al. (2018) reported strong oxygen and pH gradients with depth in TL.

Two sedimentary facies were observed, the lower one at 57–35 cm and an upper one subdivided into an intermediate interval (35–19 cm) and upper interval (19–0 cm) (text-figs. 2, 6). The lower facies consisted of laminated sediments characteristic of fluvial seasonal variations and non-bioturbation. The mud content was somewhat variable in the lower facies, ranging from <60–100%, but was consistently near 100% through the intermediate interval, increasing again in variability in the upper interval. The TOC varied between ~6–9% in the lower facies, dropped dramatically to ~1% in the intermediate interval, then increased to ~6% in the upper interval. The temporal distribution of Re was consistent with TOC, with very low values in the intermediate interval and higher, variable values in the lower and upper facies. The intermediate and upper intervals appeared to be non-laminated, although this could be an overexposure artifact in the radiograph due to ice in the core. The high concentration of Al, Fe, and peak mud content associated with strong declines in TOC, Re, and Li, indicated an interval of high terrigenous sedimentation at 35–19 cm.

The most notable characteristic of the core was the consistency of the following features in the 35–19 cm core interval. The TOC, Re and Li dropped, mud was quite stable, while Cu, Zn, Ni, Fe, V, Al, $F2_{Tess}$-Cu, $F2_{Tess}$-Zn, and $F2_{Tess}$-Fe all increased (text-fig. 6). As noted in the discussion of TLCI07, PTEs can be adsorbed or sequestered by Fe/Mn oxi-hydroxides, as well as with Fe sulfides (e.g., pyrite), both serving as "sinks" that greatly reduces PTE bioavailability (Martínez-Colón et al. 2009; Martínez-Colón et al. 2018). This interpretation was supported by the rapid increase in bulk concentrations of Cu, Zn, Ni, and V at the 35–19 cm interval, paralleling the temporal variability of Fe (text-fig. 6). Interestingly, unlike TLCI07, mud content only correlated negatively with Pb, As and Se. However, the lack of positive correlations between other PTEs and mud may be an artifact of the dominance of mud throughout the core, even though the mud was consistently highest in the 35–19 cm interval.

Also notable were the negative correlations of Cu, Zn, Ni, Fe, and V with TOC and CO_3, indicating that organic matter and

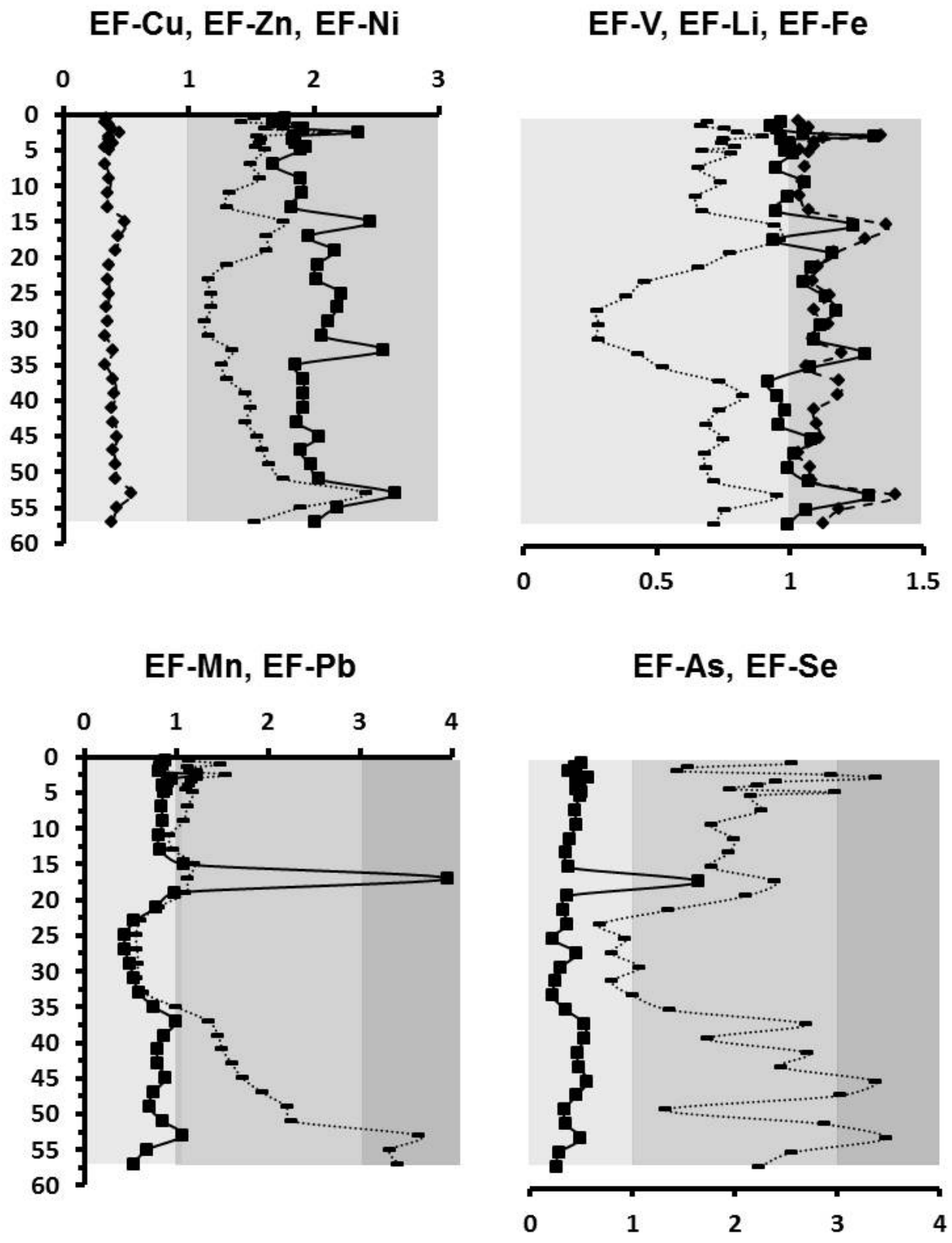

TEXT-FIGURE 7
Vertical distributions of EF (enrichment factors) in sediment core TLCI09. Range values: "no enrichment" (very light gray); "minor enrichment" (light gray); "moderate enrichment" (gray). Square, dash, and diamond symbols represent the first, second and third PTE in each panel.

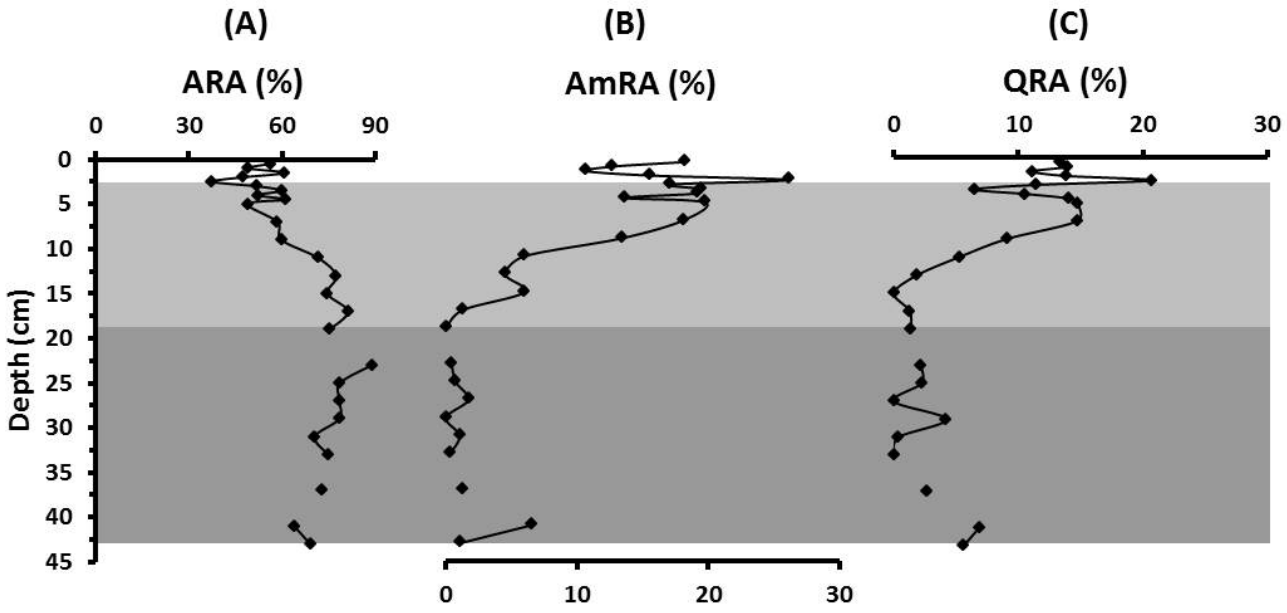

TEXT-FIGURE 8
Temporal distribution of key foraminiferal taxa relative abundances in Core TLCI07. A: ARA (*A. beccarii*), AmRA (*A. agglutinans*), and QRA (*Q. rhodiensis*). Light gray bar: interval of higher sedimentation. Dark gray bar: interval of anoxic conditions.

carbonate were not functioning as PTE "sinks". Interestingly, Pb, Li, and Se positively correlated with TOC, which potentially increased their bioavailability for benthic foraminifers as discussed by Martínez-Colón et al. (2018). Overall, the highest bulk concentrations for most PTEs were found in the intermediate facies (35–19 cm) intimately associated with Fe as the dominant "sink". The $F2_{Tess}$-Cu, $F2_{Tess}$-Zn, and $F2_{Tess}$-Fe bioavailable PTEs show a discernable increase at 35–19 cm depth (text-fig. 6).

The successful dating of core TLCI09 above 25 cm depth provided insight into the timing of the lower and upper facies changes. Most PTEs rapidly increased in concentration during the late 1800's, reaching maximum values at 25 cm (ca. 1908). The subsurface peaks may indicate pollution and watershed changes associated with agriculture in the late 19th and early 20th centuries. A rapid decrease in PTE concentrations occurred above 19 cm (ca. 1962). Webb and Gómez-Gómez (1998) documented a temporal decrease in As from 1925–1995 from sediment cores. They also reported an increase in Pb during the same time interval, while we recorded relative stability in Pb concentrations above 35 cm depth in TLCI09.

Puerto Rico was annexed by the USA in 1898. During the 20th century, the SJBE, including TL, experienced two pulses of urbanization. The first began in the late 1930's with migration from rural areas to the cities. When Puerto Rico became a US-Commonwealth in 1952, urbanization increased exponentially. Webb and Gómez-Gómez (1998) specifically noted that extensive pasture and forest areas in the SJBE watershed underwent housing and commercial development between 1900 and 1970.

As with TLCI07, PTE enrichment was surprisingly minimal. Most PTEs either exhibited "no enrichment" (Ni, Li, Mn, As) or "minor enrichment" (Cu, Zn, V, Fe, Se), indicating no substantial change in PTE pollution over time. Lead actually decreased from core-base up to 29 cm, changing from "moderate enrichment" and remaining mostly with "minor enrichment" towards core-top.

Foraminiferal Distributions

The dominant assemblage throughout the core is composed of *Q. seminula*, *A. beccarii*, and *Q. rhodiensis*. These species have been reported in environments with high TOC in tropical settings (e.g., Seiglie 1968; Donnici et al. 2012). In field experiments, *Q. seminula* has been found to thrive in anoxic environments by exhibiting an exponential growth at the initial stages of anoxia followed by a decrease over time (Langlet et al. 2014). This species previously has been reported associated with disturbed environments such as beneath shrimp ponds (Debenay et al. 2009) and on fresh volcanic ash (Hess and Kuhnt 1996). As 42% of the subsamples in this core were devoid of foraminiferal tests and 15% of subsamples had <10 tests/sample, interpretations are primarily restricted to variability in preservation potential of foraminiferal tests within the core. This scenario was also observed in a core collected in TL in 2005 in which samples were barren at depths >16 cm (Martínez-Colón and Hallock 2010). The prevalence of barren samples more likely reflects lack of preservation than changes in sedimentation/erosion within the drainage basin. The interpretation of post-depositional dissolution was based on the low CO_3 values (<5%), absence of ostracods, lack of correlation with most PTEs/TOC, and evidence of etching and corrosion in some of the specimens recovered. Dissolution scars of benthic

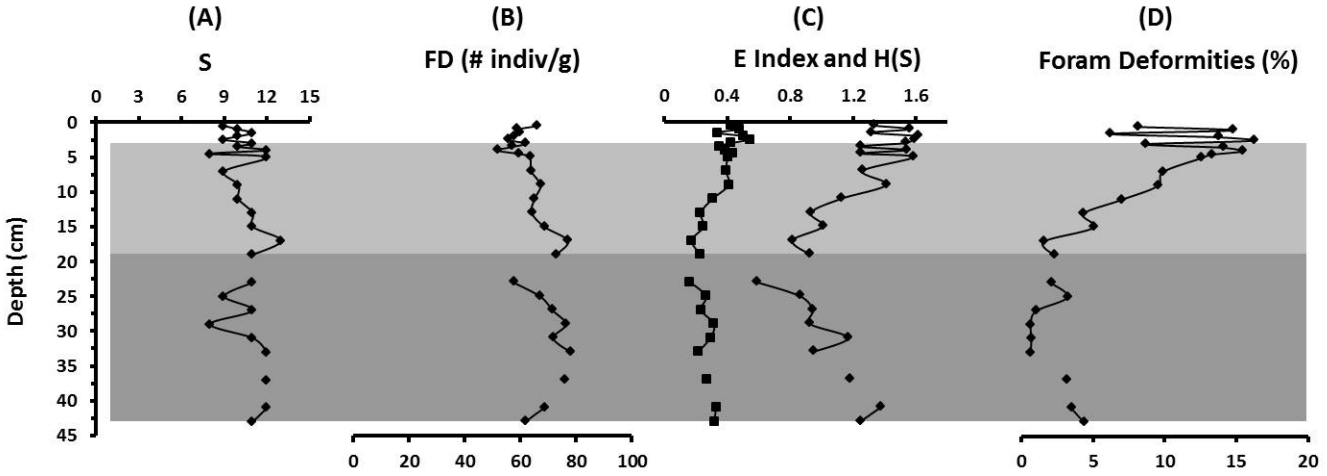

TEXT-FIGURE 9
Vertical distributions of foraminiferal ecological parameters in Core TLCI07. A: S (Number of Species), B: FD (Foraminiferal Density), C: H(S) (Shannon Index) (diamonds), E (Equitability Index) (squares). Light gray bar: interval of higher sedimentation. Dark gray bar: interval of anoxic conditions.

foraminifers have been ascribed to chemically and domestically polluted estuaries (e.g., Al-Azmel et al. 2009; Martínez-Colón et al. 2010) as well as in pH culture experiments (Le Cadre et al. 2003).

Comparison of TLCI07 and TLCI09 Cores

The two cores were collected in rather different environmental conditions. TLCI07 was collected from an open lagoon location at a water depth of less than a meter, where surface sediments were well oxygenated. In contrast, TLCI09 was collected in an enclosed location at 12 m depth, in anoxic conditions (sampling station #19- Martínez-Colón et al. 2018). Thus, the physical and chemical conditions were quite different. These differences can explain some of the important variabilities between the sedimentological aspects of the cores. For example, while TLCI07 sediments were predominantly muddy, the mud content varied from ~40–80%. In contrast, the TLCI09 sediments were completely mud dominated, especially in the middle and upper parts of the core. The opposite trend was seen in CO_3. In TLCI07, CO_3 ranged from ~5–30%, though it was lowest in the upper facies. In TLCI09, there were virtually no carbonates, likely reflecting dissolution.

A striking similarity between the cores was in the zones of higher terrigenous influence (text-fig. 3), in which mud was highest, CO_3 and TOC were lowest, bulk concentrations of Cu, Zn, Ni, Fe, V and Al were consistently highest, and Re was consistently lowest (text-figs. 4, 6). Interestingly, that zone was first encountered a few centimeters below the surface in TLCI07 and 19 cm below the surface in TLCI09. Are the similarities in lithology and geochemistry coincidental? Or do they represent contemporaneous deposition, with minimal sediment thickness overlying that unit in TLCI07 as a consequence of the very shallow depth from which it was collected?

The foraminiferal assemblages were more difficult to compare between cores because the densities were so low in TLCI09. The trends in TLCI07 were clear in that *Ammonia* completely dominated the lower section, while *Ammobaculites* and *Quinqueloculina* became more prevalent in the upper section, as was reflected in the H(S) and in the prevalence of DF, which were found mostly in miliolids such as *Quinqueloculina.*

Interestingly, some ecological indices (e.g., FD, S, and DF), as well as absolute abundances of certain taxa (*A. beccarii*, *A. agglutinans*, *E. discoidale*) did positively correlate with As, Li and Mn. These contaminants may behave as essential micronutrients, as noted in previous studies that documented bioaccumulated contaminants in macrobenthic organisms associated with bioavailable fractions of PTEs (Luoma and Bryan 1978; Tessier et al. 1984; Tessier and Campbell 1987).

Numerous studies have addressed the physiochemical processes that manipulate PTE fractionation and speciation in marine environments (e.g., Caplat et al. 2005; Gree-Ruíz 2005; Marínez-Colón et al. 2009). Other studies have established protocols for PTE extractions from sediments, assuming the degree of bioavailability based on the operational sequence of extractions. Tessier et al. (1979) proposed that PTEs can exists in five different fractions ranging from most bioavailable (fraction 1: exchangeable) to the least bioavailable (fraction 5: residual). However, bioavailability based upon macroinvertebrates may not extrapolate to benthic foraminifers appropriately due to basic biological differences (Martínez-Colón et al. 2018). This scenario has led to discrepancies in interpretations when assessing the impact of PTEs on benthic foraminifers. As recommended by Martínez-Colón et al. (2009, 2018), fractionation and sequential extraction procedures are essential, as is recognizing that correlation does not imply causation. Recognizing the physiochemical conditions (historical if possible) in which foraminifers were exposed, as well as the conditions that can determine the speciation, fractionation, and bioavailability of PTEs, is essential to valid interpretations. Based upon observations from this study and from Martínez-Colón et al. (2018), we

conclude that the $F2_{Tess}$ acid-soluble fraction (second most bioavailable according to Tessier et al. 1979; Tessier and Campbell 1987) is not a satisfactory choice to indicate bioavailability for benthic foraminifers. The PTEs locked in the crystalline structure of $CaCO_3$ minerals (e.g., calcite, malachite, cerussite) are not bioavailable to foraminifers. It is important to consider the actual biological significance of sediment-bound PTEs in relation to foraminifers and fractionation. Thus, we further conclude that specific experimental studies will be essential to determine what fractions of sediment-associated PTEs can be taken up by benthic foraminifers.

CONCLUSIONS

Two cores provide information on the temporal variability of environmental conditions in TL as it relates to the impact of PTEs on benthic foraminiferal assemblages. The two cores reflect different environmental conditions within the lagoon that could influence sedimentation rates and sources of pollution. Oxygenation and sediment characteristics have been influenced by changes in terrigenous input since the early 1900s, which have in turn influenced the variability and fractionation of PTEs. Enrichment factors indicate minimal enrichment in the sediment cores assessed. Statistical correlations suggest that mud and Fe (e.g., Fe oxides) are major "sink" mechanisms for most PTEs, thereby reducing their bioavailability in the water columnb and in sediments in the case of Fe. The PTEs adsorbed to mud (exchangeable fraction) are likely to be bioavailable for benthic foraminifers..

The foraminiferal assemblage dominated by *A. beccarii*, *A. agglutinans*, *Q. rhodiensis*, and *Q. seminula,* coupled with very low densities and diversities, are indicative of stressed environmental conditions. Key foraminiferal taxa and ecological indices exhibited negative correlations with some bulk PTE concentrations, but very limited correlations with selected acid-soluble fractions ($F2_{Tess}$-Cu, $F2_{Tess}$-Zn, $F2_{Tess}$-Fe) assumed to be bioavailable based upon studies of macroinvertebrates. Based upon this discrepancy, we recognize the need to better understand what PTE fractions hold biological significance for foraminifers. In addition, we recommend not considering the $F2_{Tess}$-bioavailable fraction as an adequate indicator of bioavailability for benthic foraminifers in environmental assessments.

ACKNOWLEDGMENTS

The authors would like to thank Dr Jorge Bauzá, Mrs Adelís Cabán and Gladys Rivera from the San Juan Bay Estuary system for their field support. ICONOS images from Torrecillas Lagoon were provided by the Geological and Environmental Remote Sensing Laboratory from the University of Puerto Rico-Mayaguez Campus. Special thanks to Humberto Bojórquez-Leyva from Universidad Nacional Autónoma de México's Institute of Marine Science and Limnology for his Atomic Adsorption Spectroscopy training and to Mrs. Molly R. McLaughlin from the USGS Coastal and Marine Science Center in St Petersburg, Florida, for field equipment and freeze drying. Special thanks to technicians from the Manatí Medical Center in Puerto Rico for taking the core radiographs. We will like to acknowledge the helpful comments of Dr. Letizia Di Bella, Dr. Guillem Mateu-Vicens, and Dr. Lamidi Babalola. This work was supported by Puerto Rico Sea Grant (grant number R-21-1-08) and the USA Geological Survey Cooperative Agreement (grant number 99HQAG0004).

REFERENCES

ABRAHIM, G. M. S. and PARKER, R. J., 2008. Assessment of heavy metal enrichment factors and the degree of contamination in marine sediments from Tamaki Estuary, Auckland, New Zealand. *Environmental Monitoring and Assessment*, 136: 227–238.

ABU-ZEID, R. H., BASAHAM, A. S. and EL SAYED, M. A., 2013. Effect of municipial wastewaters on bottom sediment geochemistry and benthic foraminifera of two Red Sea coastal inlets, Jeddah, Saudi Arabia. *Environmental Earth Sciences*, 68: 451–469.

ACEVEDO-FIGUEROA, D. JIMENEZ, B. D. and RODRIGUEZ-SIERRA, C., 2006. Trace metals in sediments of two estuarine lagoons from Puerto Rico. *Environmental Pollution*, 141: 336–342.

ALVE, E., 1995. Benthic foraminiferal responses to estuarine pollution: a review. *Journal of Foraminiferal Research*, 25: 190–203.

———, 1991. Benthic foraminifera in sediment cores reflecting heavy metal pollution in Sørfjord, western Norway. *Journal of Foraminiferal Research*, 21: 1–19.

AL-ZAMEL, A. Z., AL-SARAWI, M. A., KHADER, S. R. and AL-RIFAIY, I. A., 2009. Benthic foraminifera from polluted marine environment of Sulaibikhat Bay (Kuwait). *Environmental Monitoring and Assessment*, 149: 395–409.

APPLEBY, P. G., 1992. Chronostratigraphic techniques in recent sediments. In: Smol, J. P., Birks, H. J. B., and Last, W. M. Eds., Uranium-series Disequilibrium: Applications to Earth, Marine and Environmental Sciences, 171–203. New York: Kluwer Academic Press.

ARSLAN, M., KAMINSKI, M.A., KHALIL, A. and TAWABINI, B.S., 2017. Benthic Foraminifera in Eastern Bahrain: Relationship to local pollution sources. *Polish Journal of Environmental Sciences,* 26 (3), 969–984.

BACON, J. R. and DAVIDSON, C. M., 2008. Is there a future for sequential chemical extraction? *Analyst*, 133: 25–46.

BADAWI, A. and EL-MENHAWEY, W., 2016. Tolerance of benthic foraminifera to anthropogenic stressors from three sites of the Egyptian coasts. *The Egyptian Journal of Aquatic Research*, 42: 49–56.

BALACHANDRAN, K. K., LAKURAJ, C. M., MARTIN, G. D., SRINIVAS, K. and VENUGOPAL, P., 2006. Environmental analysis of heavy metal deposition in a flow-restricted tropical estuary and its adjacent shelf. *Environmental Forensics*, 7: 345–351.

BERGIN, F., KUÇUKSEZGIN, F., ULUTURHAN, E., BARUT, I., MERIÇ, E., AVŞAR, N. and NAZIK, A., 2006. The response of benthic foraminifera and ostracoda to heavy metal pollution in Gulf of Izmir (Eastern Aegean Sea). *Estuaries and Coastal Shelf Science*, 66: 368–386.

BOUCHET, V. M. P., ALVE, E., RYGG, B. and TELFORD, R. J., 2012.Benthic foraminifera provide a promising tool for ecological quality assessment of marine waters. *Ecological Indicators,* 23: 66–75.

BREITHAUPT, J. L., SMOAK, J. M., SMITH, T. J. and SANDERS, C. J., 2014. Temporal variability of carbon and nutrient burial, sediment accretion, and mass accumulation over the past century in a carbonate platform mangrove forest of the Florida Everglades. *Journal of Geophysical Research: Biogeosciences*, 119: 2032–2048.

BROOKS, G. R., DEVINE, B., LARSON, R. A. and ROOD, B. P., 2007. Sedimentary Development of Coral Bay, St. John, USVI: A shift from natural to anthropogenic influences. *Caribbean Journal of Science*, 43: 226–243.

BUNCH, B.W., CERCO, C.F., DORTH, M.S., JOHNSON B.H. and KIM, K.W., 2000. Hydrodynamic and water quality model of San Juan Bay estuary, Technical Report ERDC TR-00-1, U.S. Army Corps of Engineer Waterways Experiment Station. Vicksburg, Mississippi, USA.

BUZAS-STEPHENS, P. and BUZAS, M. A., 2005. Population dynamics and dissolution of foraminifera in Nueces Bay, Texas. *Journal of Foraminiferal Research*, 35: 248–258.

CAPLAT, C., TEXIER, H., BARILLIER, D., and LELIEVRE, C., 2005. Heavy metals mobility in harbour contaminated sediments: the case of Port-en-Bessin. *Marine Pollution Bulletin*, 50: 504–511.

CLARKE, K.R. and GORLEY, R.N., 2006. PRIMER v6: User Manual/Tutorial PRIMER-E, Plymouth.

DALE V. H. and BEYEL, S. C., 2001. Challenges in the development and use of ecological indicators. *Ecological Indicators*, 1: 3–10.

DAVIES, B. E., BOWMAN, C., DAVIES, T. C. and SELINUS, O., 2005. Medical Geology: perspectives and prospects. In: Selinus, O., Alloway, B., Centeno, J. A., Finkelman, R. B., Fuge, R., Lindh, U., and Smedley, P., Eds., *Essentials of Medical Geology*, 1–41. New York: Elsevier Academic Press.

DEBENAY, J.-P., PATRONA, D. and GOGUENHEIM, H., 2009. Colonization of coastal environments by foraminifera: insight from shrimp ponds in New Caledonia (SW Pacific). *Journal of Foraminiferal Research*, 39: 249–266.

DONNICI, S., SERANDREI-BARBERO, R., BONARDI, M. and SPERLE, M., 2012. Benthic foraminifera as proxies of pollution: The case of Guanabara Bay (Brazil). *Marine Pollution Bulletin*, 64: 2015–2028.

EKENGELE, N. L., MYUNG, C. J., OMBOLO, A., NGOUNOU, N., EKODECK, G. and MBOME, L., 2008. Metals pollution in freshly deposited sediments from river Mingoa, main tributary to the municipal lake of Yaounde, Cameron. *Geosciences Journal*, 12: 337–347.

ELLIS, S.R. 1976. History of dredging and filling of lagoons in the San Juan area, Puerto Rico. *U.S. Geological Survey Water-Resources Investigations Report*, 38: 76p.

ELLIS, S. R. and GÓMEZ-GÓMEZ, F., 1976. Hydrologic characteristics of lagoons at San Juan, Puerto Rico, during a January 1974 tidal cycle. U*.S. Geological Survey Water-Resources Investigations*, 38: 52p.

EMRICH, K., MARTÍNEZ-COLÓN, M. and ALEGRÍA, H., 2017. Is untreated sewage impacting coral reefs in Caye Caulker, Belize? *Journal of Foraminiferal Research*, 47: 20–33.

FONTANIER, C., FABRI, M.-C., BUSCAIL, R., BISCARA, L., KOHO, K., REICHART, G.J., COSSA, D., GALAUP, S., CHABAUD, G., and PIGOT, L., 2012. Deep-sea foraminifera from the Cassidaigne Canyon (NW Mediterranean): Assessing the environmental impact of bauxite red mud disposal. *Marine Pollution Bulletin*, 64: 1895–1910.

FOSTER, W. J., ARMYNOT DU CHÂTELET, E. and ROGERSON, M., 2012. Testing benthic foraminiferal distributions as a contemporary quantitative approach to biomonitoring estuarine heavy metal pollution. *Marine Pollution Bulletin*, 64: 1039–1048.

FRONTALINI, F. and COCCIONI, R., 2008. Benthic foraminifera for heavy metal pollution monitoring: A case study from the central Adriatic Sea coast of Italy. *Estuarine Coastal and Shelf Science*, 74: 404–417.

GESLIN, E., BARRAS, C., LANNGLET, D., NARDELLI, M. P., KIM, J-H., BONNIN, J., METZGER, E. and JORISSEN, F. J., 2014. Survival, reproduction and calcification of three benthic foraminiferal species in response to experimentally induced hypoxia. In: Kitazato H., and Bernhard, J. M., Eds., *Approaches to Study Living Foraminifera*, 163–193. Tokyo: Springer.

GÓMEZ-GÓMEZ, F., QUIÑONES, F. and ELLIS, S.R., 1983, Hydrologic characteristics of lagoons at San Juan, Puerto Rico, during and October 1974 tidal cycle: U.S. Geological Survey Open-File Report 82–349, 34 pp.

GREEN-RUÍZ, C., RUELAS-INZUNZA, J. and PÁEZ-OSUNA, F., 2005. Mercury in surface sediments and benthic organism from Guaymas Bay, east coast of the Gulf California. *Environmental Geochemistry and Health*, 27: 321–329.

GREEN-RUÍZ, C., 2005, Adsorption of mercury (II) from aqueous solutions by the clay mineral montmorillonite. *Bulletin of Environmental Contamination and Toxicology*, 75: 1137–1142.

HESS, S. and KUHNT, W., 1996. Deep-sea benthic foraminiferal recolonization of the 1991 Mt. Pinatubo ash layer in the South China Sea. *Marine Micropaleontology*, 28: 171–197.

JORISSEN, F. J., 1999. Benthic foraminiferal microhabitats below the sediment-water interface. In: Sen Gupta, B. K., Ed., *Modern Foraminifera,* 179–191. Boston: Kluwer Academic Publishers.

KALAIVANAN, R., JAYAPRAKASH, M., NETHAJI, S., ARYA, V. and GIRIDHARAN, L., 2017. Geochemistry of core sediments from tropical mangrove region of Tamil Nadu: implications on trace metals. *Journal of Earth Science and Climate Change*, doi:10.4172/5127–7617.10000385.

KFOURI, P. B. P., FIGUEIRA, R. C. L., FIGUEIREDO, A. M. G., SOUZA, S. H. M. and EICHLER, B. B., 2005. Metal levels and foraminifera occurrence in sediment cores from Guanabara Bay, Rio de Janeiro, Brazil. *Journal of Radioanalytical and Nuclear Chemistry*, 265: 459–466.

LANGLET, D., BAAL, C., GESLIN, E., METZGER, E., ZUSCHIN, M., RIEDEL, B., RISGAARD-PETERSEN, N., STACHOWITSCH, M. and JORISSEN, F. J., 2014. Foraminiferal species responses to in situ, experimentally induced anoxia in the Adriatic Sea. *Biogeosciences*, 11: 1775–1797.

LARSON, R. A., BROOKS, G. R., DEVINE, B., SCHWING, P. T., HOLMES, C. W., JILBERT, T. and REICHART, G-J., 2015. Elemental signature of terrigenous sediment runoff as recorded in coastal salt ponds: US Virgin Islands. *Applied Geochemistry*, 65: 573–585.

LE CADRE, V., DEBENAY, J.-P. and LESOURD, M., 2003. Low pH effects on *Ammonia beccarii* test deformation: Implications for using test deformation as a pollution indicator. *Journal of Foraminiferal Research*, 33: 1–9.

LEE, S. V. and CUNDY, A. B., 2001. Heavy metal contamination and mixing processes in sediments from the Humber Estuary, Eastern England. *Estuarine and Coastal Shelf Science*, 53: 619–636.

LOEBLICH, A.R. and TAPPAN, H., 1987. *Foraminiferal genera and their classification.* New York: Van Nostrand Reinhold Company.

LONG, E.R., MACDONALD, D.D., SMITH, S.L. and CALDER, F.D., 1995. Incidence of adverse biological effects within ranges of chemical concentrations in marine and estuarine sediments. *Environmental Management*,19: 81–97.

LING, S. D., SINCLAIR, M., LEVIS, C. J., REEVES, S. E. and EDGAR, G. J., 2017. Ubiquity of microplastics in coastal seafloor sediments. *Marine Pollution Bulletin*, 121: 10–110.

LUOMA, S. N. and BRYAN, G. W., 1978. Factors controlling the availability of sediment-bound lead to the estuarine bivalve *Scrobicularia plana*. *Journal of the Marine Biological Association of the U.K.*, 58: 793–802.

MARTÍNEZ-COLÓN, M. and HALLOCK, P., 2010. Preliminary survey on Foraminiferal Responses to pollutants in Torrecillas Lagoon Puerto Rico. *Caribbean Journal of Science*, 46: 1–6.

MARTÍNEZ-COLÓN, M., HALLOCK, P. and GREEN-RUÍZ, C., 2009. Strategies for using shallow-water benthic foraminifers as bioindicators of potentially toxic elements: a review. *Journal of Foraminiferal Research*, 39: 278–299.

MARTÍNEZ-COLÓN, M. and HALLOCK, P. and GREEN-RUÍZ, C. and SMOAK, J. M., 2018. Benthic foraminiferal as bioindicators of potentially toxic elements (PTE) pollution: Torrecilla Lagoon, Puerto Rico. *Ecological Indicators Journal*, 89: 516–257.

MARTINS, V. A., FRONTALINI, F., TRAMONTE, K. M., FIGUEIRA, R. C., MIRANDA, P., SEQUEIRA, C., FERNANDEZ-FERNANDEZ, S., DIAS, J. A., YAMASHITA, C., RENO, R., LAUT, L. L., SILVA, F. S., RODRIGUES, M. A., BERNARDES, C., NAGAI, R., SOUSA, S. H., MAHIQUES, M., RUBIO, B., BERNABEU, A., REY, D. and ROCHA, F., 2013. Assessment of the health quality of Ria de Aveiro (Portugal): heavy metals and benthic foraminifera. *Marine Pollution Bulletin*, 70: 18–33.

MARTINS, V. A., SILVA, F., LAUT, L. L. M., FRONTALINI, F., CLEMENTE, I. M. M. M., MIRANDA, P., FIGUEIRA, R., SOUSA, S. H. M. and DIAS, J. M. A., 2015. Response of benthic foraminifera to organic matter quantity and quality and bioavailable concentrations of metals in Aveiro Lagoon (Portugal). *PLoS ONE*, doi:10.1371/journal.pone.0118077.

MARTINS, V. A., YAMASHITA, C., SOUSA, S. H. M., MARTINS, P., LAUT, L. L. M., FIGUEIRA, R. C. L., MAHIQUES, M. M., FERREIRA DA SILVA, E., ALVEIRINHO DIAS, J. M. and ROCHA, F., 2011.The response of benthic foraminifera to pollution and environmental stress in Ria de Aveiro (N Portugal) La respuesta de los foraminíferos bentónicos a la contaminación y el estrés ambiental en la Ría de Aveiro (N de Portugal). *Journal of Iberian Geology*, 37: 231–246.

MATEU-VICENS, G., KHOKHLOVA, A. and SEBASTIAN-PASTOR, T., 2014. Epiphytic foraminiferal indices as bioindicators in Mediterranean seagrass meadows. *Journal of Foraminiferal Research*, 44: 325–339.

MURRAY, J. W., 1991. *Ecology and paleoecology of benthonic foraminifera*. UK/New York: Longman Scientific and Technical/Wiley, 397 pp.

PARKER, W. C. and ARNOLD, A. J., 1999. Quantitative methods of data analysis in foraminiferal ecology. In Sen Gupta, B.K., Ed., *Modern Foraminifera*, 71–89. Boston: Kluwer Academic Publishers.

PINTO, E., 2003. Heavy metal-induced oxidative stress in algae. *Journal of Phycology*, 39: 1008–1018.

PINTO, R., PATRICIO, J., BAETA, A., FATH, B. D., NETO, J. M. and MARQUES, J. C., 2009. Review and evaluation of estuarine biotic indices to assess benthic condition. *Ecological Indicators*, 9: 1–25.

POAG, W., 1981. *Ecologic Atlas of Benthic Foraminifera of the Gulf of Mexico*. Hutchinson Ross Publishing Company, 256pp.

RAO, K. K. and RAO, T. S., 1979. Studies on pollution ecology of Foraminifera of the Trivandrum coast. *Indian Journal of Marine Science*, 8: 31–35.

SCHAFER, C. T., COLLINS, E. S. and SMITH, J. N., 1991. Relationship of Foraminifera and thecamoebian distributions to sediments contaminated by pulp mill effluent: Saguenay Fiord, Quebec, Canada. *Marine Micropaleontology*, 17: 255–283.

SCHINTU, M., MARRUCCI, A., MARRAS, B., GALGANI, F., BUOSI, C., IBBA, A. and CHERCHI, A., 2016. Heavy metal accumulation in surface sediments at the port of Cagliari (Sardinia, western Mediterranean): Environmental assessment using sequential extraction and benthic foraminifera. *Marine Pollution Bulletin*, 111: 45–56.

SCHÖNFELD, J., ALVE, E., GESLIN, E., JORISSEN, F., KORSUN, K., SPEZZAFERRI, S., ABRAMOVICH, S., ALMOGI-LABIN, A., ARMYNOT DU CHATELET, E., BARRAS, C., BERGAMIN, L., BICCHI, E., BOUCHET, V., CEARRETA, A., DI BELLA, L., DIJKSTRA, N., DISARO, S. T., FERRARO, L., FRONTALINI, F., GENNARI, G., GOLIKOVA, E., HAYNERT, K., HESS, S., HUSUM, K., MARTINS, V., MCGANN, M., ORON, S., ROMANO, E., SOUSA, S. M. and TSUJIMOTO, A., 2012. The FOBIMO (FOraminiferal BIo-MOnitoring) initiative-Towards a standardized protocol for soft-bottom benthic foraminiferal monitoring studies. *Marine Micropaleontology*, 94: 1–13.

SEIGLIE, G. A., 1968. Foraminiferal assemblages as indicators of high organic carbon content in sediments and polluted waters. *American Association of Petroleum Geologists Bulletin*, 52: 2231–2241.

———, 1971. A preliminary note on the relationships between foraminifers andpollution in two Puerto Rican bays. *Caribbean Journal of Science*, 1: 93–98.

———, 1974. Foraminifers of Mayaguez and Añasco Bays and its surroundings, Part 4: relationships of foraminifers and pollution in Mayaguez Bay. *Caribbean Journal of Science*, 14: 1–68.

———, 1975a. Late Holocene changes on the Foraminiferal assemblages of Jobos Bay and surroundings, Puerto Rico. Aguirre Power Project, Environmental Studies Jobos Bay Puerto Rico Final Report, Puerto Rico Nuclear Center #196.

———, 1975b. Foraminifers of Guayanilla Bay and their use as environmental indicators. *Revista Española de Micropaleontología*, 7: 453–487.

SEN GUPTA, B. K., 2013. The roots of environmental micropalaeontology: early inquiries into modern foraminiferal distributions. In: Bowden, A. J., Gregory, F. J. and Henderson, A. S., Eds., *Landmarks in foraminiferal micropalaeontology: History and Development,* 181–191. London: The Micropalaeontological Society, Special Publications.

SEN GUPTA, B. K., TURNER, R. E. and RABALAIS, N. N., 1996. Seasonal oxygen depletion on continental-shelf waters of Louisiana: Historical records on benthic foraminifera. *Geology*, 24: 227–230.

SESHAN, B. R. R., NATESAN, U. and DEEPTHI, K., 2010. Geochemical and statistical approach for evaluation of heavy metal pollution in core sediments in southeast coast of India. *International Journal of Environmental Science and Techonology*, 7: 291–306.

SHARMA, S. and CHATTERJEE, S., 2017. Microplastic pollution, a threat to marine ecosystem and human health: a short review. *Environmental Science and Pollution Research*, 24: 21530–21547.

SMOAK, J. M., BREITHAUPT, J. L., SMITH III, T. J. and SANDERS, C. J., 2013.Sediment accretion and organic carbon burial relative to

sea-level rise and storm events in two mangrove forest in Everglades National Park. *Catena*, 104: 58–66.

TESSIER, A. and CAMPBELL, P. G. C., 1987. Partitioning of trace metals in sediments: Relationships with bioavailability. *Hydrobiologia*, 149: 43–52.

TESSIER, A. and CAMPBELL, P. G. C., AUCLAIR, J. C. and BISSON, M., 1984. Relationships between the partitioning of trace metals in sediments and their accumulation in the tissues of the freshwater mollusc *Elliptio complanata* in a mining area. *Canadian Journal of Fisheries and Aquiatic Sciences*, 41: 1463–1472.

TESSIER, A. and CAMPBELL, P. G. C., and BISSON, M., 1979. Sequential extraction procedure for the speciation of particulate trace metals. *Analytical Chemistry*, 51: 844–581.

UNLU, S., ALPAR, B., AYDIN, S., AKBULAK, C., BALKIS, N., BARUT, I., MERIC, E., AKSU, A., and KIRBASOGLU, C., 2006. Anthropogenic pollution in sediments from the Gulf of Gemlik (Marmara Sea, Turkey); Cause-result relationship. *Fresenius Environmental Bulletin*, 15: 1521–1530.

WEBB, R.M.T. and GÓMEZ-GÓMEZ, F., 1998. Synoptic survey of water quality and bottom sediments, San Juan Bay Estuary System, Puerto Rico, December 1994–July 1995. *U.S.G.S. Water Resources Investigations Report* 97-4144, 69 pp.

YANKO, V., AHMAD, M. and KAMINSKI, M., 1998. Morphological deformities of benthic foraminiferal tests in response to pollution by heavy metals: implications for pollution monitoring. *Journal of Foraminiferal Research*, 28: 177–200.

YANKO, V., KONDARIUK, T. and MOTNENKO, I., 2017. Benthic Foraminifera indicate environmental stress from river discharge to marine ecosystems: Example from the Black Sea. *Journal of Foraminiferal Research*, 47: 70–92.

ZIMMERMAN, A. J. and WEINDORF, D. C., 2010. Heavy metal and trace metal analysis in soil by sequential extraction: A review of procedures. *International Journal of Analytical Chemistry*, 2010: 1–7.

ZITELLO, A. G., WHITALL, D. R., DIEPPA, A., CHRISTENSEN, J. D., MONACO M. E. and ROHMANN, S.O., 2008. Characterizing Jobos Bay, Puerto Rico: A watershed modeling analysis and monitoring Plan. NOAA Technical Memorandum NOS NCCOS, 76, 81 pp.

APPENDIX A
Core TLCI09 Pb-210 analysis.

Core TLCI09 Pb-210 analysis.

Sample	Depth (cm)	Cumulative weight/depth (g/cm^2)	Excess Pb-210 (dpm/g)	Excess Pb-210 activity error	Age at given interval (yr)	Age 1s error	Date at given interval	Mass sedimentation rate (mg/cm^2/yr)	Binford's sedimentation rate 1s error (mg/cm^2/yr)
TLCI09#1	0–0.5	0.15	4.84	0.27	0.82	0.596	2009	179	10
TLCI09#2	0.5–1	0.37	4.17	0.18	1.91	0.605	2008	201	9
TLCI09#3	1–1.5	0.57	6.11	0.29	3.47	0.616	2006	132	6
TLCI09#4	1.5–2	0.76	5.54	0.28	4.79	0.627	2005	139	7
TLCI09#5	2–2.5	0.95	5.14	0.21	6.18	0.640	2003	144	6
TLCI09#6	2.5–3	1.18	4.80	0.27	7.72	0.652	2002	147	8
TLCI09#7	3–3.5	1.32	4.94	0.29	8.77	0.662	2001	137	8
TLCI09#8	3.5–4	1.45	4.48	0.25	9.62	0.671	2000	147	8
TLCI09#9	4–4.5	1.58	4.53	0.30	10.55	0.680	1999	141	10
TLCI09#10	4.5–5	1.72	4.25	0.17	11.50	0.692	1998	146	6
TLCI09#11	5–7	2.33	3.83	0.20	15.60	0.719	1994	150	8
TLCI09#12	7–9	2.94	4.50	0.21	21.06	0.762	1988	110	5
TLCI09#13	9–11	3.48	3.66	0.17	25.78	0.814	1984	116	6
TLCI09#14	11–13	4.24	2.81	0.14	31.71	0.880	1978	127	7
TLCI09#15	13–15	5.07	2.52	0.09	38.89	1.019	1971	116	5
TLCI09#16	15–17	5.79	2.67	0.09	47.27	1.232	1962	86	4
TLCI09#17	17–19	6.42	2.82	0.10	57.55	1.588	1952	61	3
TLCI09#18	19–21	7.24	1.92	0.10	70.68	2.186	1939	62	4
TLCI09#19	21–23	8.28	1.01	0.10	83.93	2.877	1926	78	9
TLCI09#20	23–25	9.46	0.75	0.07	101.82	4.501	1908	66	9
TLCI09#21	25–27	10.64	0.69	0.10	139.84	10.02	1870	31	8
TLCI9#22–#36	No dates recorded from TLCI09#22–#36.								

APPENDIX B

Core TLCI07 PTE analysis. Concentrations are in mg/kg except for percent (%) (*). EF-ME: enrichment factor of metal (has no units). F2-PTE: acid-soluble PTE.

PTE	Cu	EF-Cu	F2-Cu	Zn	EF-Zn	F2-Zn	Ni	EF-Ni
DL	0.20	-	0.20	0.20	-	0.20	0.50	-
TLCI07#1	38.30	1.52	8.40	62.60	1.18	15.75	13.70	0.36
TLCI07#2	37.90	1.47	8.31	61.50	1.13	15.73	13.30	0.34
TLCI07#3	32.60	1.41	6.98	53.20	1.09	14.68	11.90	0.34
TLCI07#4	29.90	1.43	7.73	49.40	1.12	15.78	11.40	0.36
TLCI07#5	32.50	1.33	6.91	57.00	1.10	14.61	12.60	0.34
TLCI07#6	31.50	1.30	6.95	52.70	1.03	14.06	12.80	0.35
TLCI07#7	43.50	0.98	6.46	79.50	0.85	14.03	18.90	0.28
TLCI07#8	39.90	1.09	7.11	68.20	0.89	14.14	16.20	0.29
TLCI07#9	40.00	1.10	7.00	74.80	0.97	13.77	16.80	0.31
TLCI07#10	45.20	1.19	6.91	83.60	1.04	14.61	19.00	0.33
TLCI07#11	51.20	1.16	7.24	86.80	0.93	13.69	21.40	0.32
TLCI07#12	65.40	1.46	9.47	86.70	0.92	15.09	22.70	0.34
TLCI07#13	88.00	1.61	11.22	103.00	0.89	15.68	28.00	0.34
TLCI07#14	79.00	1.67	15.80	95.20	0.95	17.31	24.20	0.34
TLCI07#15	63.70	1.56	14.04	82.20	0.96	16.63	23.80	0.39
TLCI07#16	58.00	1.53	11.34	72.80	0.91	15.55	20.40	0.36
TLCI07#17	38.80	1.56	11.59	103.00	1.96	15.80	15.70	0.42
TLCI07#18	55.00	1.72	9.72	71.00	1.05	14.81	19.40	0.40
TLCI07#19	55.70	1.68	8.74	72.90	1.04	14.97	19.40	0.39
TLCI07#20	57.50	1.72	10.50	72.40	1.02	15.07	20.70	0.41
TLCI07#21	57.10	2.18	9.18	72.40	1.31	13.57	21.20	0.54
TLCI07#22	56.90	1.77	9.45	69.20	1.02	13.81	21.00	0.43
TLCI07#23	54.90	1.73	8.01	78.60	1.17	13.51	20.50	0.43
TLCI07#24	52.40	1.75	6.16	66.80	1.06	11.39	20.80	0.46
TLCI07#25	49.60	1.88	7.13	56.00	1.00	12.34	19.40	0.49
TLCI07#26	53.30	1.69	3.38	64.00	0.96	10.44	21.50	0.45
TLCI07#27	35.10	1.58	2.20	46.20	0.98	9.28	14.30	0.43
TLCI07#28	32.50	1.39	1.50	46.90	0.95	8.60	13.20	0.37
TLCI07#29	45.40	1.70	2.02	57.50	1.02	7.93	18.60	0.46

PTE	Pb	EF-Pb	As	EF-As	Li	EF-Li	Se	EF-Se
DL	0.50	-	0.10	-	0.50	-	0.10	-
TLCI07#1	11.80	1.06	18.90	2.60	19.70	0.53	1.10	1.69
TLCI07#2	18.60	1.63	18.70	2.52	20.10	0.53	0.50	1.15
TLCI07#3	12.80	1.25	16.50	2.48	17.50	0.52	1.70	15.63
TLCI07#4	16.60	1.78	14.60	2.42	16.00	0.52	1.30	5.70
TLCI07#5	59.80	5.50	18.00	2.55	18.00	0.50	1.30	2.72
TLCI07#6	9.10	0.85	14.40	2.06	17.90	0.50	1.20	2.65
TLCI07#7	12.80	0.65	13.20	1.03	39.40	0.60	1.20	4.91
TLCI07#8	13.10	0.81	14.10	1.34	31.20	0.58	1.30	3.83
TLCI07#9	24.40	1.51	13.80	1.31	34.30	0.64	0.70	3.09
TLCI07#10	12.90	0.76	13.50	1.23	40.00	0.72	0.90	3.49
TLCI07#11	17.40	0.88	15.10	1.18	43.90	0.68	1.00	3.60
TLCI07#12	21.40	1.08	14.80	1.14	53.50	0.81	0.50	3.47
TLCI07#13	12.00	0.49	14.40	0.91	69.80	0.87	0.80	7.62
TLCI07#14	11.30	0.54	14.60	1.07	62.40	0.90	1.20	3.29
TLCI07#15	10.20	0.56	16.10	1.37	54.60	0.91	0.40	2.81
TLCI07#16	10.40	0.62	15.50	1.41	45.60	0.82	1.20	3.64
TLCI07#17	7.20	0.65	14.70	2.04	33.90	0.93	0.80	1.69
TLCI07#18	11.40	0.80	18.50	2.00	42.80	0.91	1.00	2.11
TLCI07#19	12.20	0.83	19.60	2.05	44.20	0.91	1.00	2.11
TLCI07#20	9.80	0.66	19.50	2.02	47.80	0.97	1.30	2.74
TLCI07#21	6.80	0.58	27.40	3.63	45.10	1.18	0.70	1.48
TLCI07#22	11.80	0.83	28.30	3.04	43.90	0.93	0.30	0.63
TLCI07#23	6.60	0.47	29.50	3.22	42.10	0.90	0.60	1.27
TLCI07#24	5.50	0.41	35.30	4.09	41.50	0.95	0.90	1.90
TLCI07#25	9.50	0.81	36.30	4.75	35.10	0.91	0.70	1.48
TLCI07#26	9.50	0.68	35.30	3.87	40.70	0.88	1.00	2.11
TLCI07#27	10.10	1.02	25.80	4.02	21.10	0.65	0.90	1.90
TLCI07#28	10.30	0.99	22.50	3.33	22.00	0.64	0.60	1.27
TLCI07#29	7.60	0.64	33.00	4.28	32.90	0.84	1.10	2.32

PTE	Fe*	EF-Fe	F2-Fe*	Mn	EF-Mn	V	EF-V
DL	0.01	-	0.01	1.00	-	1.00	-
TLCI07#1	5.21	0.10	0.96	1270.00	1.37	93.00	1.28
TLCI07#2	6.28	0.12	0.40	516.00	0.49	99.00	1.33
TLCI07#3	1.61	0.19	0.31	137.00	0.89	91.00	1.37
TLCI07#4	3.73	0.21	0.45	937.00	2.90	81.00	1.34
TLCI07#5	4.25	0.11	0.95	3020.00	4.46	94.00	1.33
TLCI07#6	4.92	0.14	0.59	1460.00	2.28	107.00	1.53
TLCI07#7	3.48	0.18	0.65	767.00	2.21	212.00	1.65
TLCI07#8	4.14	0.15	0.59	947.00	1.97	169.00	1.60
TLCI07#9	2.61	0.15	0.51	592.00	1.84	199.00	1.89
TLCI07#10	2.32	0.11	0.42	598.00	1.64	237.00	2.15
TLCI07#11	3.64	0.17	0.37	830.00	2.11	238.00	1.86
TLCI07#12	0.76	0.07	0.62	299.00	1.47	150.00	1.16
TLCI07#13	0.63	0.08	0.48	248.00	1.67	171.00	1.08
TLCI07#14	3.16	0.11	0.47	1080.00	2.09	149.00	1.09
TLCI07#15	0.94	0.08	0.48	435.00	2.15	123.00	1.05
TLCI07#16	4.13	0.16	0.70	920.00	1.97	132.00	1.20
TLCI07#17	2.73	1.15	0.13	867.00	2.02	84.00	1.17
TLCI07#18	2.76	2.02	0.20	735.00	2.98	116.00	1.26
TLCI07#19	5.07	1.09	0.15	666.00	0.80	112.00	1.17
TLCI07#20	4.29	1.04	0.18	656.00	0.88	117.00	1.21
TLCI07#21	4.78	1.01	0.20	1470.00	1.73	123.00	1.63
TLCI07#22	0.62	0.62	0.09	352.00	1.95	122.00	1.31
TLCI07#23	3.46	1.32	0.17	1870.00	3.97	121.00	1.32
TLCI07#24	2.68	1.50	0.12	739.00	2.30	131.00	1.52
TLCI07#25	2.75	1.29	0.02	645.00	1.69	121.00	1.58
TLCI07#26	1.89	1.24	0.11	727.00	2.64	126.00	1.38
TLCI07#27	3.93	1.78	0.15	830.00	2.09	93.00	1.45
TLCI07#28	3.48	1.64	0.12	741.00	1.94	88.00	1.30
TLCI07#29	4.06	1.54	0.14	964.00	2.03	115.00	1.49

Core TLCI09 PTE analysis. Concentrations are in MG/KG except for percent (%) (*). EF-ME: enrichment factor of metal (has no units). F2-PTE: acid-soluble PTE.

PTE	Cu	EF-Cu	F2-Cu	Zn	EF-Zn	F2-Zn	Ni	EF-Ni
DL	0.20	-	0.20	0.20	-	0.20	0.50	-
TLCI09#1	57.00	1.77	13.60	104.00	1.53	57.12	16.90	0.35
TLCI09#2	56.80	1.67	26.20	102.00	1.42	51.20	17.60	0.34
TLCI09#3	54.90	1.75	8.98	124.00	1.87	55.01	17.40	0.37
TLCI09#4	58.60	1.92	8.90	104.00	1.61	43.42	18.20	0.39
TLCI09#5	57.50	2.36	8.11	108.00	2.10	56.77	17.00	0.46
TLCI09#6	63.20	1.84	11.43	112.00	1.54	65.57	19.30	0.37
TLCI09#7	61.60	1.83	9.50	112.00	1.57	53.42	18.70	0.37
TLCI09#8	57.00	1.85	8.81	102.00	1.57	46.46	18.60	0.40
TLCI09#9	63.40	1.93	8.05	106.00	1.53	41.68	16.90	0.34
TLCI09#10	59.20	1.90	ND	106.00	1.61	ND	17.70	0.38
TLCI09#11	61.10	1.67	8.79	115.00	1.49	56.79	18.70	0.34
TLCI09#12	63.80	1.89	15.55	112.00	1.57	47.23	19.20	0.38
TLCI09#13	79.20	1.91	11.20	116.00	1.32	56.74	22.70	0.36
TLCI09#14	70.50	1.82	10.98	107.00	1.31	63.17	21.00	0.36
TLCI09#15	72.50	2.45	14.54	110.00	1.76	51.00	22.40	0.50
TLCI09#16	61.40	1.96	24.65	107.00	1.62	53.74	21.30	0.45
TLCI09#17	76.90	2.16	10.48	122.00	1.62	46.28	22.60	0.42
TLCI09#18	101.00	2.02	13.45	138.00	1.31	74.84	28.40	0.38
TLCI09#19	111.00	2.02	22.64	134.00	1.15	73.51	29.70	0.36
TLCI09#20	125.00	2.22	ND	140.00	1.18	ND	31.30	0.37
TLCI09#21	123.00	2.19	ND	140.00	1.18	ND	29.90	0.35
TLCI09#22	119.00	2.12	40.99	134.00	1.13	68.23	31.00	0.36
TLCI09#23	116.00	2.06	28.48	137.00	1.15	66.60	28.90	0.34
TLCI09#24	114.00	2.56	18.33	127.00	1.35	67.33	27.00	0.40
TLCI09#25	81.30	1.86	12.48	117.00	1.26	63.47	22.80	0.34
TLCI09#26	69.30	1.92	ND	99.60	1.30	ND	22.00	0.40
TLCI09#27	66.10	1.91	5.58	106.00	1.45	51.84	21.90	0.42
TLCI09#28	68.80	1.91	14.58	114.00	1.50	68.36	21.40	0.39
TLCI09#29	68.10	1.86	14.56	112.00	1.45	62.25	22.50	0.41
TLCI09#30	67.80	2.04	23.94	109.00	1.55	66.88	22.00	0.44
TLCI09#31	65.60	1.89	22.77	116.00	1.58	79.26	21.00	0.40
TLCI09#32	78.40	1.97	4.99	138.00	1.64	73.38	25.50	0.42
TLCI09#33	69.00	2.03	3.98	126.00	1.76	67.83	21.90	0.43
TLCI09#34	57.10	2.64	27.26	110.00	2.41	71.62	18.00	0.55
TLCI09#35	64.20	2.19	23.40	117.00	1.89	75.96	19.20	0.43
TLCI09#36	80.60	2.01	2.05	129.00	1.52	74.68	23.70	0.39

PTE	Pb	EF-Pb	As	EF-As	Li	EF-Li	Se	EF-Se
DL	0.50	-	0.10	-	0.50	-	0.10	-
TLCI09#1	16.40	1.14	4.70	0.50	32.70	0.69	1.10	2.56
TLCI09#2	22.50	1.49	4.30	0.44	33.20	0.67	0.70	1.54
TLCI09#3	15.70	1.13	3.40	0.38	34.60	0.75	0.60	1.44
TLCI09#4	15.70	1.15	4.00	0.45	36.10	0.80	1.20	2.94
TLCI09#5	16.80	1.55	4.00	0.57	32.10	0.90	1.10	3.38
TLCI09#6	17.90	1.17	4.50	0.45	37.70	0.75	1.10	2.40
TLCI09#7	17.50	1.17	4.80	0.49	36.90	0.75	1.00	2.23
TLCI09#8	15.70	1.15	4.00	0.45	35.80	0.79	0.80	1.95
TLCI09#9	16.20	1.11	4.80	0.51	32.20	0.67	1.30	2.97
TLCI09#10	16.50	1.19	4.40	0.49	35.60	0.78	0.90	2.16
TLCI09#11	18.20	1.12	4.60	0.44	35.20	0.66	1.10	2.26
TLCI09#12	16.20	1.08	4.40	0.45	36.70	0.74	0.80	1.77
TLCI09#13	17.10	0.93	4.60	0.38	39.30	0.65	1.10	1.99
TLCI09#14	16.70	0.97	3.90	0.35	38.20	0.67	1.00	1.94
TLCI09#15	15.80	1.20	3.20	0.37	41.00	0.94	0.70	1.77
TLCI09#16	15.60	1.12	14.90	1.65	44.30	0.96	1.00	2.39
TLCI09#17	17.50	1.11	3.70	0.36	40.50	0.78	1.00	2.11
TLCI09#18	17.90	0.81	4.60	0.32	47.90	0.65	0.90	1.35
TLCI09#19	14.90	0.61	5.80	0.36	36.50	0.45	0.50	0.68
TLCI09#20	14.10	0.56	3.60	0.22	31.90	0.39	0.70	0.93
TLCI09#21	14.40	0.58	7.30	0.45	22.90	0.28	0.60	0.80
TLCI09#22	14.60	0.58	4.90	0.30	23.40	0.28	0.80	1.07
TLCI09#23	14.40	0.58	4.10	0.25	23.10	0.28	0.60	0.80
TLCI09#24	12.80	0.65	2.80	0.22	28.10	0.43	0.60	1.01
TLCI09#25	19.40	1.00	4.50	0.36	33.60	0.52	0.80	1.37
TLCI09#26	21.70	1.35	5.60	0.54	39.00	0.74	1.30	2.70
TLCI09#27	22.40	1.46	5.30	0.53	41.80	0.82	0.80	1.73
TLCI09#28	24.10	1.50	4.80	0.46	38.80	0.73	1.30	2.70
TLCI09#29	26.20	1.61	5.10	0.48	36.90	0.69	1.20	2.46
TLCI09#30	25.50	1.72	5.40	0.56	36.70	0.75	1.50	3.38
TLCI09#31	29.90	1.94	4.50	0.45	34.70	0.68	1.40	3.03
TLCI09#32	39.00	2.21	3.90	0.34	39.90	0.68	0.70	1.32
TLCI09#33	34.00	2.26	3.40	0.35	35.70	0.72	1.30	2.87
TLCI09#34	34.90	3.64	3.10	0.50	30.20	0.95	1.00	3.47
TLCI09#35	43.40	3.33	2.40	0.28	32.60	0.76	1.00	2.55
TLCI09#36	61.00	3.42	3.00	0.26	42.30	0.72	1.20	2.24

PTE	Fe*	EF-Fe	F2-Fe*	Mn	EF-Mn	V	EF-V
DL	0.01	-	0.01	1.00	-	1.00	-
TLCI09#1	3.49	1.03	1.53	536.00	0.88	90.00	0.96
TLCI09#2	3.73	1.04	2.10	554.00	0.86	91.00	0.93
TLCI09#3	3.52	1.07	1.31	492.00	0.83	86.00	0.95
TLCI09#4	3.4	1.06	1.07	473.00	0.82	93.00	1.05
TLCI09#5	3.44	1.34	1.35	566.00	1.23	93.00	1.32
TLCI09#6	4.06	1.13	1.50	618.00	0.95	96.00	0.97
TLCI09#7	3.85	1.09	1.23	580.00	0.91	97.00	1.00
TLCI09#8	3.52	1.09	1.00	498.00	0.86	89.00	1.00
TLCI09#9	3.56	1.03	0.98	557.00	0.90	93.00	0.98
TLCI09#10	3.51	1.07	ND	510.00	0.86	91.00	1.01
TLCI09#11	4.05	1.06	1.16	578.00	0.84	100.00	0.95
TLCI09#12	3.71	1.05	1.44	548.00	0.86	103.00	1.05
TLCI09#13	4.52	1.04	1.38	635.00	0.81	119.00	0.99
TLCI09#14	4.35	1.07	1.52	604.00	0.83	106.00	0.95
TLCI09#15	4.23	1.36	1.33	606.00	1.08	106.00	1.24
TLCI09#16	4.21	1.28	1.99	2340.00	3.95	85.00	0.94
TLCI09#17	4.34	1.16	1.05	664.00	0.99	119.00	1.16
TLCI09#18	5.78	1.10	1.82	746.00	0.79	156.00	1.08
TLCI09#19	6.27	1.09	2.14	568.00	0.55	167.00	1.05
TLCI09#20	6.78	1.15	ND	476.00	0.45	184.00	1.13
TLCI09#21	6.43	1.09	ND	472.00	0.44	191.00	1.18
TLCI09#22	6.76	1.15	2.56	523.00	0.49	181.00	1.11
TLCI09#23	6.39	1.08	2.32	576.00	0.54	177.00	1.09
TLCI09#24	5.59	1.19	2.12	500.00	0.59	165.00	1.28
TLCI09#25	4.87	1.06	1.62	631.00	0.76	136.00	1.07
TLCI09#26	4.49	1.18	ND	680.00	1.00	96.00	0.92
TLCI09#27	4.28	1.18	1.40	566.00	0.87	95.00	0.95
TLCI09#28	4.12	1.09	2.17	543.00	0.80	102.00	0.98
TLCI09#29	4.23	1.10	1.72	554.00	0.80	101.00	0.95
TLCI09#30	3.88	1.11	1.83	556.00	0.88	104.00	1.08
TLCI09#31	3.75	1.03	2.24	494.00	0.75	102.00	1.02
TLCI09#32	4.49	1.08	1.36	531.00	0.71	114.00	0.99
TLCI09#33	3.84	1.08	1.14	549.00	0.86	105.00	1.07
TLCI09#34	3.16	1.39	1.99	437.00	1.07	81.00	1.30
TLCI09#35	3.64	1.18	2.15	378.00	0.68	90.00	1.06
TLCI09#36	4.74	1.13	1.58	410.00	0.54	115.00	0.99

APPENDIX C

Core TLCI07. Pearson correlation matrix of PTEs of interest, acid-soluble (carbonate) bioavailable PTEs (F2-bioavailable), TOC, CO_3, and mud (N = 29; grey = significant positive correlation; red = significant negative correlation; $p<0.05$ [0.37]).

	Cu	F2-Cu	Zn	F2-Zn	Ni	Pb	As	Li	Se	Fe	F2-Fe	Mn	V	TOC	CO_3	Mud
Cu																
F2-Cu	**0.47**															
Zn	**0.73**	**0.62**														
F2-Zn	0.20	**0.93**	**0.46**													
Ni	**0.96**	0.34	**0.75**	0.06												
Pb	-0.28	0.07	-0.12	0.29	-0.32											
As	0.12	**-0.46**	-0.30	**-0.66**	0.17	**-0.46**										
Li	**0.94**	**0.40**	**0.81**	0.13	**0.98**	-0.31	0.07									
Se	0.09	-0.26	-0.02	**-0.41**	0.21	**-0.55**	**0.63**	0.12								
Fe	**0.58**	0.12	**0.57**	0.00	**0.71**	-0.07	0.04	**0.68**	**0.40**							
F2-Fe	0.31	**0.88**	**0.42**	**0.82**	0.16	-0.03	-0.25	0.22	-0.23	-0.04						
Mn	-0.02	**0.45**	-0.06	**0.55**	-0.18	0.34	**-0.51**	-0.16	**-0.58**	-0.29	**0.43**					
V	**0.44**	0.12	**0.57**	0.07	**0.58**	0.10	-0.30	**0.58**	0.17	**0.91**	-0.15	-0.19				
TOC	**-0.51**	**-0.66**	**-0.68**	**-0.56**	**-0.48**	-0.13	**0.53**	**-0.56**	**0.40**	-0.33	**-0.45**	-0.29	**-0.45**			
CO_3	-0.08	-0.17	-0.34	-0.27	-0.16	**-0.45**	**0.56**	-0.19	0.10	**-0.44**	0.18	0.02	**-0.68**	0.20		
Mud	0.35	0.21	**0.47**	0.14	**0.40**	-0.04	**-0.38**	**0.39**	0.06	**0.41**	-0.11	-0.02	**0.60**	-0.30	**-0.63**	

APPENDIX D

Core TLCI09. Pearson correlation matrix of PTEs of interest, acid-soluble (carbonate) bioavailable PTEs (F2-bioavailable), TOC, CO_3, and mud (N = 36; grey = significant positive correlation; red = significant negative correlation; $p<0.05$ [0.32]).

	Cu	F2-Cu	Zn	F2-Zn	Ni	Pb	As	Li	Se	Fe	F2-Fe	Mn	V	TOC	CO_3	Mud
Cu																
F2-Cu	-0.06															
Zn	**0.82**	-0.22														
F2-Zn	-0.28	**0.65**	-0.19													
Ni	**0.95**	-0.04	**0.81**	-0.20												
Pb	-0.23	-0.14	0.08	0.28	-0.09											
As	0.07	0.00	-0.08	**-0.32**	0.16	**-0.35**										
Li	**-0.41**	-0.06	-0.28	**0.41**	-0.23	0.26	0.10									
Se	**-0.49**	0.00	**-0.43**	0.26	**-0.44**	**0.41**	0.02	**0.32**								
Fe	**0.97**	-0.04	**0.78**	-0.26	**0.95**	-0.28	0.21	**-0.34**	**-0.53**							
F2-Fe	0.03	**0.85**	-0.02	**0.80**	0.10	0.20	-0.12	0.07	0.05	0.07						
Mn	-0.04	0.21	-0.14	0.07	0.07	**-0.34**	**0.77**	**0.38**	0.01	0.09	0.11					
V	**0.98**	-0.08	**0.80**	-0.31	**0.91**	-0.30	0.06	**-0.45**	**-0.50**	**0.95**	-0.01	-0.07				
TOC	**-0.83**	0.04	**-0.64**	**0.41**	**-0.71**	**0.48**	-0.12	**0.70**	**0.63**	**-0.82**	0.06	0.07	**-0.84**			
CO_3	**-0.67**	-0.06	**-0.56**	0.26	**-0.55**	0.30	-0.01	**0.53**	**0.40**	**-0.64**	-0.01	0.11	**-0.71**	**0.71**		
Mud	0.18	-0.15	0.06	-0.22	0.07	**-0.58**	0.17	-0.13	**-0.34**	0.23	-0.24	0.26	0.23	**-0.38**	-0.19	

APPENDIX E

Core TLCI07 samples foraminiferal raw counts. Gray bar: barren samples unless otherwise noted. **: species not present in at least 5% of the samples.

Sample	TLCI07 #1	TLCI07 #2	TLCI07 #3	TLCI07 #4	TLCI07 #5	TLCI07 #6	TLCI07 #7	TLCI07 #8	TLCI07 #9	TLCI07 #10	TLCI07 #11
Ammonia beccarii	114	116	148	110	83	136	138	114	148	126	155
Ammobaculites agglutinans	37	30	26	36	58	45	45	42	33	51	48
Brizalina sp.	0	0	0	0	0	0	0	0	0	0	0
Cornuspira sp.	0	0	1	1	0	0	2	1	0	0	0
Discorbinella sp.	0	0	0	2	0	0	0	1	0	2	0
Elphidium sp.	0	4	0	2	7	3	0	3	8	4	2
Elphidium crispum	1	1	1	0	0	1	1	0	0	2	0
E.discoidale	11	15	9	14	7	9	7	5	8	9	7
*E. fibriatulum***	0	0	0	0	0	0	0	0	0	0	0
E. poeyanum	0	0	0	3	2	4	2	2	2	6	5
Fursenkoina sp.	0	0	0	0	0	0	0	0	0	0	1
Florilus grateloupi	1	3	2	0	0	2	2	3	0	1	3
Miliolinella sp.	0	1	0	0	0	1	0	0	1	0	0
Quinqueloculina sp.	6	6	0	12	12	10	5	8	0	7	5
Q. agglutinans	0	0	1	0	0	0	0	2	0	0	0
Q. rhodiensis	27	33	27	32	46	30	15	23	34	38	39
Q. linneiana	1	0	2	0	0	0	0	0	0	0	0
Q. candeiana	0	0	0	0	0	0	0	0	0	0	0
Rosalina sp.	0	0	1	0	0	0	0	0	0	0	0
Triloculina sp.	5	22	25	20	6	22	6	15	8	10	0
T. trigonula	0	0	0	0	1	0	0	0	0	2	0
Deformed Foram.	18	41	36	37	43	25	38	4	37	37	29
Total forams	**203**	**231**	**243**	**232**	**222**	**263**	**223**	**219**	**242**	**258**	**265**
S	9	10	11	10	9	11	10	12	8	12	9
FD	66	58	60	58	56	62	55	52	59	63	64
H(S)	1.33	1.56	1.31	1.61	1.59	1.53	1.24	1.54	1.25	1.58	1.26
E	0.42	0.48	0.34	0.50	0.54	0.42	0.35	0.39	0.44	0.40	0.39
Subsample (g)	3.09	4.02	4.08	4.02	4.00	4.25	4.05	4.24	4.07	4.07	4.15

Sample	TLCI07 #12	TLCI07 #13	TLCI07 #14	TLCI07 #15	TLCI07 #16	TLCI07 #17		TLCI07 #19	TLCI07 #20	TLCI07 #21	TLCI07 #22	TLCI07 #23
Ammonia beccarii	165	191	206	212	255	223		207	213	230	243	203
Ammobaculites agglutinans	37	16	12	17	4	0		1	2	5	0	3
Brizalina sp.	0	0	0	2	3	6		4	0	4	7	0
Cornuspira sp.	0	0	0	1	0	0		0	0	0	0	2
Discorbinella sp.	0	0	0	0	2	1		1	0	0	0	0
Elphidium sp.	3	7	2	3	1	1		0	5	4	8	6
Elphidium crispum	0	1	1	0	0	1		0	0	0	0	0
E.discoidale	12	14	11	21	18	32		1	26	20	18	17
*E. fibriatulum***	0	0	0	0	1	0		0	0	0	0	0
E. poeyanum	11	3	5	5	4	3		0	12	10	9	19
Fursenkoina sp.	0	0	0	0	0	0		2	0	1	0	0
Florilus grateloupi	0	6	3	4	7	1		3	1	6	0	11
Miliolinella sp.	0	0	0	0	0	0		0	0	0	0	0
Quinqueloculina sp.	6	0	0	9	3	15		5	5	10	6	0
Q. agglutinans	0	0	0	0	0	0		0	0	0	0	0
Q. rhodiensis	25	14	5	0	4	4		5	6	0	13	1
Q. linneiana	0	0	0	0	0	0		0	0	0	0	0
Q. candeiana	0	0	1	0	0	0		0	1	1	0	0
Rosalina sp.	1	1	0	2	0	0		1	0	0	0	2
Triloculina sp.	12	11	15	0	1	0		0	0	0	0	13
T. trigonula	4	0	1	3	4	4		3	0	2	6	7
Deformed Foram.	29	20	12	15	5	7		5	9	0	2	2
Total forams	**276**	**264**	**262**	**279**	**307**	**291**		**233**	**271**	**293**	**310**	**284**
S	10	10	11	11	13	11		11	9	11	8	11
FD	67	64	63	67	75	71		58	67	72	76	71
H(S)	1.41	1.12	0.93	1.01	0.81	0.92		0.59	0.86	0.94	0.92	1.17
E	0.41	0.31	0.23	0.25	0.17	0.23		0.16	0.26	0.23	0.32	0.29
Subsample (g)	4.11	4.11	4.15	4.14	4.07	4.07		4.05	4.04	4.09	4.06	4.02

TLCI07#18

Sample	TLCI07 #24		TLCI07 #26		TLCI07 #28	TLCI07 #29
Ammonia beccarii.	236		221		177	197
Ammobaculites agglutinans	1		4		18	3
Brizalina sp.	3		3		0	0
Cornuspira sp.	0		1		0	0
Discorbinella sp.	0		0		0	0
Elphidium sp.	4		6		19	9
Elphidium crispum	1		0		1	1
E.discoidale	28		15		9	9
*E. fibriatulum***	0		0		0	0
E. poeyanum	17		21		17	24
Fursenkoina sp.	0		0		0	0
Florilus grateloupi	3	TLCI07#25	6	TLCI07#27	6	9
Miliolinella sp.	0		0		0	0
Quinqueloculina sp.	4		6		4	5
Q. agglutinans	0		0		0	0
Q. rhodiensis	0		8		19	16
Q. linneiana	0		0		0	0
Q. candeiana	0		0		1	0
Rosalina sp.	1		0		0	0
Triloculina sp.	6		8		2	9
T. trigonula	2		5		2	3
Deformed Foram.	2		10		10	13
Total forams	**306**		**304**		**277**	**285**
S	12		12		12	11
FD	76		76		68	62
H(S)	0.95		1.18		1.37	1.25
E	0.22		0.27		0.33	0.32
Subsample (g)	4.04		4.01		4.04	4.62

APPENDIX F

Core TLCI07. Pearson correlation matrix of bulk PTEs of interest, bioavailable PTEs ($F2_{Tess}$), foraminifers, TOC, mud, CO_3, diversity indices, percent deformed foraminifers, and relative abundance of key taxa (N=29; gray= significant positive correlation; red= significant negative correlation; $p<0.05$ [0.37]). S (Species richness). FD (Foraminiferal density). H(S) (Shannon Index). E (Equitability Index). DF (Percent deformed foraminifers). ARA (*A.* relative abundance). QRA (*Q.* relative abundance). AmRA (*A.* relative abundance).

Sample	Cu	F2-Cu	Zn	F2-Zn	Ni	Pb	As	Li	Se	Fe	F2-Fe	Mn	V	TOC	CO_3	Mud
Ammonia beccarii	**0.65**	0.17	**0.38**	-0.13	**0.65**	**-0.71**	**0.48**	**0.66**	0.33	0.19	0.24	-0.26	-0.03	-0.13	0.32	-0.01
Ammobaculites agglutinans	**-0.42**	-0.05	-0.19	0.24	**-0.42**	**0.64**	**-0.64**	**-0.44**	-0.26	0.00	-0.22	**0.39**	0.27	0.04	**-0.55**	0.30
Brizalina sp.	0.25	0.21	0.20	0.01	0.28	**-0.39**	**0.40**	0.30	0.16	0.00	0.33	-0.22	-0.21	-0.13	0.36	**-0.44**
Cornuspira sp.	-0.11	-0.05	-0.06	0.02	-0.04	-0.13	0.02	-0.06	0.28	0.07	-0.04	-0.27	0.05	0.15	0.01	-0.06
Discorbinella sp.	-0.17	0.16	0.03	0.26	-0.16	0.00	-0.35	-0.08	**-0.41**	-0.16	0.16	-0.04	0.02	-0.22	-0.05	-0.02
Elphidium sp.	0.02	**-0.52**	-0.23	**-0.60**	0.08	0.06	0.43	0.04	0.07	0.02	**-0.45**	-0.21	-0.02	0.35	0.04	0.02
E. crispum	-0.20	-0.18	0.00	-0.09	-0.21	-0.23	-0.14	-0.21	0.12	-0.05	-0.22	-0.03	0.01	0.18	0.02	0.21
E. discoidale	0.22	0.30	0.20	0.12	0.20	**-0.44**	0.29	0.19	0.27	-0.14	**0.39**	-0.18	-0.27	0.17	0.18	0.15
E. poeyanum	0.30	**-0.42**	-0.05	**-0.65**	**0.40**	**-0.46**	**0.69**	0.34	**0.45**	0.13	**-0.39**	**-0.50**	0.00	0.31	0.17	0.09
Fursenkoina sp.	0.18	0.08	0.13	0.05	0.18	-0.04	0.08	0.20	-0.12	0.21	0.14	0.15	0.10	-0.30	0.20	**-0.40**
Florilus grateloupi	0.33	-0.28	0.03	**-0.43**	0.35	**-0.58**	**0.47**	0.29	0.33	0.14	-0.22	-0.22	0.01	0.20	0.35	0.11
Miliolinella sp.	-0.34	-0.01	-0.21	0.09	-0.35	0.22	-0.21	-0.35	0.00	-0.09	-0.06	0.25	0.01	0.07	-0.20	0.08
Quinqueloculina sp.	**-0.39**	-0.03	-0.21	0.04	-0.33	0.10	-0.02	-0.34	-0.15	-0.34	0.06	0.13	-0.32	0.19	0.14	**-0.37**
Q. agglutinans	-0.24	-0.04	-0.16	0.05	-0.24	0.04	-0.19	-0.21	0.00	-0.02	-0.05	-0.02	0.05	-0.01	-0.13	0.05
Q. rhodiensis	**-0.56**	-0.28	-0.34	0.02	**-0.57**	**0.70**	**-0.45**	**-0.58**	-0.32	-0.12	-0.31	0.19	0.10	0.13	**-0.40**	0.05
Q. linneiana	-0.31	0.00	-0.29	0.13	**-0.41**	0.01	-0.06	**-0.43**	0.09	-0.27	0.12	0.15	-0.31	0.17	0.18	-0.06
Q. candeiana	0.19	-0.02	-0.03	-0.12	0.13	-0.23	0.13	0.18	0.00	-0.03	0.04	0.12	-0.12	0.08	0.15	-0.03
Rosalina sp.	**0.39**	0.25	0.24	0.15	0.34	-0.22	0.14	0.32	0.03	0.05	0.21	0.13	-0.03	-0.17	0.19	0.06
Triloculina sp.	-0.31	-0.13	-0.30	0.05	**-0.38**	0.20	-0.19	**-0.43**	0.07	-0.18	-0.25	-0.02	-0.04	0.17	-0.16	0.19
T. trigonula	0.35	-0.05	0.20	-0.24	**0.39**	-0.35	0.54	**0.39**	0.25	0.01	0.03	-0.33	-0.13	0.01	0.32	-0.26
FD (test/g)	**0.43**	0.06	0.21	-0.19	**0.45**	**-0.59**	**0.55**	**0.42**	**0.41**	0.06	0.15	-0.30	-0.13	0.16	0.23	0.02
ARA (%)	**0.67**	0.20	**0.40**	-0.09	**0.65**	**-0.68**	**0.38**	**0.69**	0.24	0.23	0.25	-0.20	0.01	-0.26	0.34	-0.04
QRA (%)	**-0.57**	-0.27	-0.34	0.03	**-0.58**	**0.71**	**-0.47**	**-0.58**	-0.33	-0.12	-0.31	0.19	0.10	0.11	**-0.40**	0.04
AmRA (%)	**-0.42**	-0.05	-0.19	0.24	**-0.42**	**0.64**	**-0.64**	**-0.44**	-0.26	0.00	-0.22	**0.39**	0.27	0.04	**-0.55**	0.30
DF (%)	**-0.42**	-0.07	-0.12	0.22	**-0.41**	**0.70**	**-0.68**	**-0.41**	**-0.41**	-0.04	-0.26	0.25	0.24	-0.02	**-0.58**	0.30
S	0.05	-0.21	-0.07	-0.25	0.07	**-0.52**	0.14	0.08	0.09	-0.13	-0.26	-0.19	-0.08	0.15	0.16	0.07
H(S)	**-0.61**	**-0.37**	**-0.42**	-0.11	**-0.57**	**0.47**	-0.27	**-0.63**	-0.06	-0.19	**-0.44**	0.06	0.02	**0.37**	-0.33	0.17
E	**-0.60**	-0.21	**-0.38**	0.06	**-0.59**	**0.70**	-0.34	**-0.63**	-0.19	-0.18	-0.24	0.20	0.01	0.24	-0.34	0.05

APPENDIX G
Core TLCI09 samples foraminiferal raw counts. Gray bar: Barren samples unless otherwise noted.

Sample	TLCI09 #1	TLCI09 #2	TLCI09#3	TLCI09#4	TLCI09#5	TLCI09 #6	TLCI09 #7	TLCI09 #8	TLCI09 #9	No Data	TLCI09#11	TLCI09#12	TLCI09#13	TLCI09 #14	TLCI09 #15	TLCI09 #16
Ammonia beccarii	0	5				9	8	2	8					1	0	1
Ammobaculites agglutinans	0	0				3	1	0	1					2	0	0
Bolivina sp.	0	0				0	0	0	1					0	0	15
Cornuspira sp.	0	0				0	0	0	0					0	0	1
Cyclogira planorbis	0	1				0	0	0	0					0	0	7
Elphidium sp.	0	0				0	0	0	0					0	0	1
E. crispum	0	0				0	3	0	0					0	0	0
E.discoidale	0	0				0	0	2	0					0	0	4
Fursenkoina punctata	0	0				0	0	1	0					0	0	0
Miliolinella sp.	0	0				0	0	0	0					0	0	0
Nonion sp.	0	1				0	0	1	2					0	0	6
Quinqueloculina sp.	0	0				0	1	0	0					0	0	1
Q. bosciana	0	0				0	0	4	0					0	0	9
Q. lamarkiana	1	0				0	1	0	0					2	0	0
Q. linneiana	0	0				0	0	0	0					0	0	0
Q. rhodiensis	0	26				5	2	1	1					0	1	16
Q. seminula	0	94				3	4	0	3					2	0	3
Reusella sp.	0	0				0	0	0	0					0	0	11
Rosalina sp.	0	0				0	0	0	3					0	1	0
Triloculina sp.	0	0				0	0	0	0					1	1	0
T. laevigata	0	0				1	1	0	4					0	0	45
T. oblonga	1	0				0	0	0	0					0	0	0
T. trigonula	0	0				0	0	0	0					0	0	0
Deformed Foram.	0	0				1	1	0	0					0	0	7
Total forams	**2**	**127**				**22**	**22**	**11**	**23**					**8**	**3**	**127**
S	2	5				5	8	6	8					5	3	13
FD	1	23				5	8	4	7					1	0	19
H(S)	0.69	0.75				1.41	1.77	1.64	1.82					1.56	1.10	1.99
E	1.00	0.42				0.82	0.73	0.86	0.77					0.95	1.00	0.56
Subsample (g)	3.26	5.46				4.20	2.77	2.94	3.20					9.39	7.90	6.83

Sample	TLCI09#17	TLCI09 #18	TLCI09 #19	No Data	TLCI09#21	TLCI09#22	TLCI09#23	TLCI09 #24	TLCI09 #25	No Data	TLCI09 #27	TLCI09 #28	TLCI09#29	TLCI09 #30	TLCI09 #31	TLCI09#32	TLCI09#33	TLCI09#34
Ammonia beccarii		22	63					1	11		6	3		24	2			
Ammobaculites agglutinans		2	0					0	2		8	10		0	1			
Bolivina sp.		0	1					0	0		0	0		0	0			
Cornuspira sp.		0	0					0	0		0	1		0	0			
Cyclogira planorbis		0	0					0	0		0	0		0	0			
Elphidium sp.		0	0					0	0		0	0		0	0			
E. crispum		0	0					0	0		0	0		0	0			
E.discoidale		5	0					0	1		1	1		0	1			
Fursenkoina punctata		0	0					0	0		0	0		0	0			
Miliolinella sp.		3	1					0	0		0	0		5	0			
Nonion sp.		0	0					0	0		3	0		0	0			
Quinqueloculina sp.		0	0					0	0		0	0		0	1			
Q. bosciana		2	0					0	5		1	1		5	0			
Q. lamarkiana		0	0					0	2		0	0		7	0			
Q. linneiana		0	1					0	0		0	0		0	0			
Q. rhodiensis		6	65					0	0		8	3		1	3			
Q. seminula		8	25					0	16		0	7		12	0			
Reusella sp.		0	0					0	0		0	0		0	0			
Rosalina sp.		0	0					0	0		0	0		0	0			
Triloculina sp.		0	1					0	0		0	2		0	0			
T. laevigata		1	1					0	6		11	0		0	0			
T. oblonga		0	0					0	0		0	0		0	0			
T. trigonula		0	0					0	0		0	1		0	2			
Deformed Foram.		2	4					0	0		3	1		0	0			
Total forams		**51**	**162**					**1**	**43**		**41**	**30**		**54**	**10**			
S		8	8					1	7		7	9		6	6			
FD		5	16					0	6		7	4		5	1			
H(S)		1.66	1.18					0.00	1.61		1.70	1.83		1.47	1.70			
E		0.66	0.41					1.00	0.72		0.78	0.69		0.73	0.91			
Subsample (g)		10.65	10.33					10.41	7.36		5.98	6.95		9.86	8.38			

Sample	TLCI09 #35	TLCI09 #36
Ammonia beccarii	5	3
Ammobaculites agglutinans	0	0
Bolivina sp.	0	0
Cornuspira sp.	0	0
Cyclogira planorbis	0	0
Elphidium sp.	0	0
E. crispum	0	0
E.discoidale	0	0
Fursenkoina punctata	0	0
Miliolinella sp.	0	0
Nonion sp.	0	0
Quinqueloculina sp.	0	0
Q. bosciana	0	0
Q. lamarkiana	0	0
Q. linneiana	0	0
Q. rhodiensis	1	0
Q. seminula	1	3
Reusella sp.	0	0
Rosalina sp.	0	0
Triloculina sp.	0	0
T. laevigata	0	0
T. oblonga	0	0
T. trigonula	0	0
Deformed Foram.	0	0
Total forams	**7**	**6**
S	3	2
FD	2	1
H(S)	0.80	0.69
E	0.74	1
Subsample (g)	4.39	8.50

APPENDIX H

Core TLCI09. Pearson correlation matrix of bulk PTEs of interest, bioavailable PTEs ($F2_{Tess}$), foraminifers, TOC, mud, CO_3, diversity indices, percent deformed foraminifers, and relative abundance of key taxa (N=29; gray= significant positive correlation; red= significant negative correlation; $p<0.05$ [0.31]). S (Species richness). FD (Foraminiferal density). H(S) (Shannon Index). E (Equitability Index). DF (Percent deformed foraminifers). QsRA (*Q. seminula* relative abundance). ARA (*A. beccarii* relative abundance). QRA (*Q. rhodiensis* relative abundance).

Sample	Cu	F2-Cu	Zn	F2-Zn	Ni	Pb	As	Li	Se	Fe	F2-Fe	Mn	V	TOC	CO_3	Mud
Ammonia beccarii	0.06	0.15	-0.03	0.15	0.04	-0.02	0.15	0.22	0.00	0.10	0.15	0.02	0.06	0.10	0.09	0.05
Ammobaculites agglutinans	-0.12	-0.08	-0.21	0.08	-0.08	0.02	0.12	0.26	0.18	-0.05	0.07	0.03	-0.14	0.22	**0.42**	0.07
Bolivina sp.	-0.12	0.16	-0.18	0.00	-0.04	-0.16	**0.75**	0.22	0.06	-0.03	0.10	**0.86**	-0.19	0.07	0.09	0.13
Cyclogira planorbis	-0.16	0.21	-0.21	0.00	-0.06	-0.11	**0.72**	0.23	-0.01	-0.04	0.17	**0.86**	-0.22	0.09	0.11	0.13
E. discoidale	-0.09	0.08	-0.15	0.05	0.04	-0.13	**0.44**	**0.37**	-0.02	0.00	0.06	**0.54**	-0.11	0.07	0.19	0.17
Miliolinella sp.	0.15	0.19	0.10	0.11	0.22	0.04	0.14	0.22	0.20	0.13	0.16	0.08	0.16	0.09	-0.13	-0.09
Nonion sp.	-0.26	0.02	**-0.41**	-0.04	-0.22	-0.15	**0.57**	0.20	0.03	-0.17	-0.05	**0.58**	**-0.33**	0.14	0.27	0.22
Quinqueloculina sp.	-0.18	0.08	-0.13	0.03	-0.14	-0.05	**0.34**	0.14	0.14	-0.13	0.03	0.33	-0.18	0.16	0.22	0.10
Q. bosciana	-0.16	0.12	-0.29	0.03	-0.04	-0.13	**0.50**	0.25	0.02	-0.07	0.03	**0.55**	-0.16	0.14	0.16	0.09
Q. lamarkiana	-0.14	0.12	-0.25	0.08	-0.13	-0.02	0.11	0.04	0.28	-0.13	0.04	0.01	-0.09	0.25	0.12	-0.04
Q. rhodiensis	-0.02	0.26	-0.13	0.09	0.03	-0.11	**0.43**	0.24	-0.26	0.10	0.27	**0.36**	-0.05	0.00	0.12	0.20
Q. seminula	-0.07	0.24	-0.18	0.09	-0.09	0.02	0.15	0.09	-0.11	0.01	0.24	0.10	-0.03	0.11	0.11	0.14
Rosalina sp.	-0.10	-0.07	-0.19	-0.06	-0.23	-0.13	0.02	-0.06	0.19	-0.16	-0.19	0.00	-0.13	0.07	0.10	0.17
Triloculina sp.	0.06	0.10	-0.05	0.09	0.10	-0.05	0.00	0.20	0.02	0.07	0.18	0.01	0.03	0.04	0.17	0.02
T. laevigata	-0.15	0.05	-0.26	0.00	-0.08	-0.15	**0.70**	0.28	0.03	-0.03	0.04	**0.77**	-0.21	0.15	0.25	0.16
T. trigonula	-0.08	0.16	-0.03	0.12	-0.03	0.21	0.04	0.05	**0.36**	-0.12	0.26	-0.09	-0.08	0.18	0.16	-0.12
FD (test/g)	-0.15	0.22	-0.30	0.14	-0.11	-0.04	**0.47**	**0.33**	0.00	-0.03	0.23	**0.40**	-0.17	0.20	0.28	0.16
ARA (%)	0.10	0.09	-0.03	0.23	0.07	0.17	-0.12	0.21	0.10	0.09	0.26	-0.12	0.07	0.12	0.06	-0.03
QRA (%)	-0.13	0.27	-0.23	0.15	-0.05	0.00	0.22	**0.36**	-0.04	-0.06	0.25	0.21	-0.18	0.21	0.29	0.09
QsRA (%)	-0.02	0.10	-0.09	0.18	-0.04	0.25	0.04	0.27	0.16	0.04	0.25	0.04	-0.03	0.22	0.16	-0.03
DF (%)	-0.01	0.05	-0.04	0.10	0.10	-0.12	**0.50**	**0.45**	-0.02	0.13	0.15	**0.49**	-0.05	0.09	0.28	0.18
S	-0.13	0.21	**-0.32**	0.20	-0.08	-0.01	**0.34**	**0.41**	0.13	-0.05	0.26	**0.34**	-0.17	0.27	**0.34**	0.15
H(S)	-0.19	0.15	**-0.36**	0.18	-0.13	0.02	**0.31**	**0.44**	0.21	-0.11	0.19	**0.31**	-0.22	**0.34**	**0.41**	0.13
E	-0.10	0.11	**-0.32**	0.22	-0.11	0.08	-0.02	**0.31**	0.14	-0.08	0.23	0.06	-0.15	0.24	0.26	0.15